Quasiparticle conductance-voltage characteristics for break junctions involving *d*-wave superconductors: charge-density-wave effects

IOP Publishing Journal of Physics: Condensed Matter
J. Phys.: Condens. Matter **29** (2017) 505602 (18pp) https://doi.org/10.1088/1361-648X/aa9867

Quasiparticle conductance-voltage characteristics for break junctions involving *d*-wave superconductors: charge-density-wave effects

T Ekino[1], A M Gabovich[2], Mai Suan Li[3], H Szymczak[3] and A I Voitenko[2]

[1] Hiroshima University, Graduate School of Integrated Arts and Sciences, Higashi-Hiroshima, 739-8521, Japan
[2] Institute of Physics, Nauka Ave. 46, Kyiv 03680, Ukraine
[3] Institute of Physics, Al. Lotników 32/46, PL-02-668 Warsaw, Poland

E-mail: voitenko@iop.kiev.ua

Received 19 September 2017, revised 27 October 2017
Accepted for publication 6 November 2017
Published 27 November 2017

Abstract

Quasiparticle tunnel conductance-voltage characteristics (CVCs), $G(V)$, were calculated for break junctions (BJs) made up of layered *d*-wave superconductors partially gapped by charge-density waves (CDWs). The current is assumed to flow in the *ab*-plane of electrodes. The influence of CDWs is analyzed by comparing the resulting CVCs with CVCs calculated for BJs made up of pure *d*-wave superconductors with relevant parameters. The main CDW-effects were found to be the appearance of new CVC peculiarities and the loss of CVC symmetry with respect to the *V*-sign. Tunnel directionality was shown to be one of the key factors in the formation of $G(V)$ dependences. In particular, the orientation of electrodes with respect to the current channel becomes very important. As a result, $G(V)$ can acquire a large variety of forms similar to those for tunnel junctions between superconductors with *s*-wave, *d*-wave, and mixed symmetry of their order parameters. The diversity of peculiarities is especially striking at finite temperatures. In the case of BJs made up of pure *d*-wave superconductors, the resulting CVC can include a two-peak gap-driven structure. The results were compared with the experimental BJ data for a number of high-T_c oxides. It was shown that the large variety of the observed current–voltage characteristics can be interpreted in the framework of our approach. Thus, quasiparticle tunnel currents in the *ab*-plane can be used as an additional mean to detect CDWs competing with superconductivity in cuprates or other layered superconductors.

Keywords: high-temperature superconductors, charge-density waves, quasiparticle tunneling, *d*-wave pairing, break junctions

(Some figures may appear in colour only in the online journal)

1. Introduction

The competition between superconductivity and other instabilities of the electron spectrum is a well-known phenomenon, which is interesting from both the theoretical and utilitarian viewpoints [1–17]. Such a struggle for the Fermi surface (FS) is quite ubiquitous, e.g. in layered cuprates [18–25] and iron-based superconductors [26–33] with their high critical temperatures, T_c's, and peculiar physical properties, which makes them important research objects. Layered dichalcogenides constitute another testing ground for the studies of the competition between and the coexistence of Cooper pairing and charge density waves (CDWs) [8, 15, 24, 34–42], the latter being the most typical kind of the electron spectrum instability. CDWs are accompanied by periodic (commensurate or incommensurate) crystal lattice distortions (PCLDs)

caused by Coulomb forces [43–48]. The combined manifestations of CDWs and PCLDs have been a hot research topic during the last decades.

The existence of CDWs in high-T_c oxides has been recently confirmed by various experimental methods, including direct scanning-tunnel-microscopy (STM) and x-ray diffraction ones. In particular, CDWs were revealed in hole-doped $La_{2-x}Ba_xCuO_4$ [49], $YBa_2Cu_3O_{7-\delta}$ [16, 50–60], $Bi_2Sr_{2-x}La_xCuO_{6+\delta}$ [61], $(Bi, Pb)_2Sr_2CuO_{6+\delta}$ [62], and $Bi_2Sr_2CaCuO_{8+\delta}$ [16, 56, 63–66] cuprates, as well as in electron-doped $Nd_{2-x}Ce_xCuO_4$ ones [67]. The observed CDWs have either a unidirectional (stripe-like) or a bidirectional (checkerboard-like) structure.

As a rough guide, the interplay between CDWs and superconductivity can be considered as a peculiar superposition of the mean-field orderings. However, the CDW structures are often not truly long-range ones, possibly due to the intrinsic disorder of cuprates [68–77]. Moreover, dynamical fluctuations might be essential in the description of high-T_c CDW superconductors [78–81]. The former factor was taken into account by us earlier [82–85], while studying quasiparticle tunneling in junctions involving cuprates. The calculations revealed a substantial smearing of CDW-driven peaks, in accordance with the experiment, where the apparent CDW-related energy gap values are widely scattered [70, 86–94]. Of course, a wide distribution of CDW gaps (which, in our interpretation, are no more than the famous pseudogaps [13, 17, 22, 68, 95–98]) manifests itself in other experiments dealing with high-T_c oxides as well. As for the fluctuation character of CDWs, its detection needs thorough measurements in the time domain, similar to those already made in cuprates and other superconductors [79, 99–104].

In this article, we are going to study the coexistence of superconductivity and CDWs by calculating quasiparticle current–voltage characteristics (CVCs) of the so-called break junctions (BJs) [86, 105–114]. While theoretically investigating high-T_c superconductors with CDWs, one should choose a definite symmetry for the superconducting order parameter. This is an enduring challenge, because the required experimental data are ambiguous. The majority of the researchers in the field concerned are inclined to the viewpoint that the $d_{x^2-y^2}$-symmetry describes the totality of experimental data more adequately than the conventional *s*-wave one does [115–118]. However, quasiparticle tunneling in the *c*-axis direction, i.e. perpendicular to the layers, testifies that there exists at least a small *s*-wave contribution to the actual superconducting order parameter [119–121].

Recently, an additional evidence [122] appeared supporting the isotropic-gap scenario for at least the most popular cuprate oxide $Bi_2Sr_2CaCu_2O_{8+\delta}$. Namely, the generation of terahertz ac Josephson radiation in superconducting $Bi_2Sr_2CaCu_2O_{8+\delta}$ mesas revealed a strong narrow 2.4 THz mode, which corresponds to the well-determined gap value. This feature agrees with the results of earlier phonon-spectroscopy studies on a number of Bi-based cuprates [123]. At the same time, STM measurements on well-prepared $Bi_2Sr_2CaCu_2O_{8+\delta}$ films demonstrated two-gap patterns that are most probably a consequence of CDW coexistence with superconductivity [124]. The cited authors identified the inner gap with the superconducting order parameter. The U-like shape of the corresponding conductance profile was considered to be an indicator of *s*-wave symmetry. Those results and arguments should be taken quite seriously into account, although they are not a direct proof of the purely isotropic superconductivity in cuprates.

Hereafter, in view of the long-standing controversy, we assume the superconductivity to be a merely $d_{x^2-y^2}$-wave one, fully recognizing that this choice may be only an approximation to the reality. The main reason in favor of such a choice consists in that phase-sensitive experiments testify to the *d*-wave picture [115–118]. Note that, since the conventional CDW pairing is isotropic but acts within narrow sectors of the Fermi surface (FS) [20–22, 125–135], its interplay with the *d*-wave background should lead to some pronounced effects, which, as we hope, will be easy to reveal.

Earlier we studied the quasiparticle currents $J(V)$ and their conductance spectra $G(V)$, where V is the bias voltage, for the experimental setup when the current flew in the *c*-axis direction, common for both electrodes. This type of tunneling between the *ab*-planes of oxides is incoherent, i.e. the quasiparticle momentum $\hbar\mathbf{k}$, where $\mathbf{k}$ is the quasiparticle wave vector and $\hbar$ Planck's constant, is not conserved. The obtained CVCs revealed both superconductivity- and CDW-related features [83–85]. However, the BJ tunneling in high-T_c oxides (perpendicularly to the *c*-axis) is quite different [114, 136–138], because it is concentrated in the *ab*-plane (at least predominately [139]) and should be coherent similarly to the Josephson current in the same configuration [115, 117, 140–142]. Unfortunately, this problem has not been studied properly. In particular, directionality effects [143–147] were not duly taken into account in the cited works. This statement concerns not only tunneling in the presence of CDWs but also in their absence. Therefore, here we analyzed the tunnel current and tunnel conductance for BJs including CDW and non-CDW *d*-wave superconductors in the coherent approximation. Charge and superconducting orderings were considered in the mean-field approximation, and the calculations of the *d*-wave superconducting, Δ, and dielectric (CDW), Σ, order parameters were carried out self-consistently [148].

The calculations were made for both the checkerboard and unidirectional CDWs, the results differing mainly quantitatively. CVCs for CDW-free *d*-wave superconductors were used as a reference point to distinguish CDW-driven effects. The latter are also interesting *per se*, since layered pure *d*-wave superconductors may be found as materials not liable to CDW-PCLD instabilities. The results described below show that the coherence of tunneling and directionality effects are crucial for the formation of CVCs in break junctions. Those CVCs do not look like textbook *s*-wave [149] or *d*-wave [150] ones. CDWs add to their complexity and, in such a way, can be detected in BJ experiments.

2. Theoretical background

2.1. Hamiltonian and order parameters

Our mean-field treatment is based on the theoretical model suggested earlier for d-wave superconductors partially gapped by CDWs [7, 83, 147, 148]. In this model, the superconducting order parameter is a Bardeen–Cooper–Schrieffer-like (BCS-like) $d_{x^2-y^2}$ one, whereas the CDW order parameter possesses the s-wave symmetry and appears only on the nested (dielectrized) FS sections below the critical temperature, T_s, which is usually larger than T_c. The dielectrically gapped FS portion includes either $N = 4$ (bidirectional or checkerboard structures) or 2 (unidirectional or stripe structures) sectors. Note that nematicity in high-T_c oxides is inherent not only to the CDW phenomenon. It was also found in the electron conductivity properties of $La_{2-x}Sr_xCuO_4$ at temperatures far above T_c, which are most probably even higher than that of pseudogap appearance [151].

The Hamiltonian of the $d_{x^2-y^2}$-wave superconductor with CDWs (dSCDW) has the form

$$H = H_{\rm kin} + H_{\rm BCS} + H_{\rm CDW}, \tag{1}$$

where

$$H_{\rm kin} = \sum_{\mathbf{k},\sigma=\uparrow,\downarrow} \sum_{i=d,nd} \xi_i(\mathbf{k}) a^\dagger_{i,\mathbf{k},\sigma} a_{i,\mathbf{k},\sigma}, \tag{2}$$

$$H_{\rm BCS} = \sum_{\mathbf{k}} \bar{\Delta}(\mathbf{k}) \sum_{i=d,nd} a^\dagger_{i,\mathbf{k},\uparrow} a^\dagger_{i,-\mathbf{k},\downarrow} + \text{c.c.}, \tag{3}$$

$$H_{\rm CDW} = \sum_{\mathbf{k},\sigma=\uparrow,\downarrow} \sum_{i=d} \bar{\Sigma}(\mathbf{k}) a^\dagger_{i,\mathbf{k},\sigma} a_{i,\mathbf{k}+\mathbf{Q},\sigma} + \text{c.c.} \tag{4}$$

Here, $\xi_i(\mathbf{k})$ is the quasiparticle spectrum in the normal phase (above the highest of the both critical temperatures, T_c and T_s); the d-wave superconducting, $\bar{\Delta}(\mathbf{k})$, and CDW (dielectric), $\bar{\Sigma}(\mathbf{k})$, order parameters are explained below; $a^\dagger$ and a are the creation and annihilation operators, respectively; σ is the quasiparticle spin projection. The CDWs are described by the vector(s) $\mathbf{Q}$, and the notations 'd' and 'nd' mark the dielectrically gapped (dielectrized) and non-gapped (non-dielectrized) FS sections, respectively.

The complex CDW order parameter equals $\Sigma_0(T)e^{i\varphi}$ (here, φ is the CDW phase). It is assumed to be $\mathbf{k}$-independent, i.e. constant (s-wave), within any of N dielectrically gapped sectors, the bisectrices of which are directed along either of the mutually perpendicular $\mathbf{k}_x$ and $\mathbf{k}_y$ axes. Each of the sectors spans the angle 2α. In the parent (non-superconducting) CDW state, the CDW order parameter magnitude $\Sigma_0(T=0) = \frac{\pi}{\gamma} T_{s0}$, where $\gamma = 1.78\ldots$ is the Euler constant, the Boltzmann constant $k_B = 1$, and $T_{s0} = T_s$, because the pure CDW state is described by the BCS-like equations of s-wave symmetry [6, 152, 153]. Therefore, the dielectric order parameter has the conventional s-wave Mühlschlegel temperature dependence

$$\Sigma_0(T) = \Sigma_0(0) \text{Mü}_s(T/T_{s0}), \tag{5}$$

where $\text{Mü}_s(x)$ is the well-known reduced ($\text{Mü}_s(0) = 1$) function. The angle θ in the two-dimensional $\mathbf{k}$-plane is reckoned from the $\mathbf{k}_x$ axis. The quantity $\bar{\Sigma}_0(T,\theta)$ spanning the whole FS can be expressed using the angular factor $f_\Sigma(\theta)$, which is equal to unity inside and zero outside each sector. Specifically, $\bar{\Sigma}_0(T,\theta)$ can be presented as follows:

$$\bar{\Sigma}_0(T,\theta) = \Sigma_0(T) f_\Sigma(\theta). \tag{6}$$

The parent pure (CDW-free) BCS $d_{x^2-y^2}$-wave superconductor (dBCS) [150] is characterized by the order parameter $\Delta_0(0)$ at $T = 0$ and the critical temperature $T_{c0} = \frac{\gamma\sqrt{e}}{2\pi}\Delta_0(0)$, where e is the base of natural logarithm. The order parameter lobes are oriented in the $\mathbf{k}_x$ and $\mathbf{k}_y$ directions, i.e. in the same (antinodal) directions as the bisectrices of CDW sectors. The profile $\bar{\Delta}_0(T,\theta)$ in the $\mathbf{k}$-space also has the factorized form

$$\bar{\Delta}_0(T,\theta) = \Delta_0(T) f_\Delta(\theta), \tag{7}$$

with another angular factor

$$f_\Delta(\theta) = \cos 2\theta. \tag{8}$$

Here,

$$\Delta_0(T) = \Delta_0(0) \text{Mü}_d(T/T_{c0}), \tag{9}$$

where $\text{Mü}_d(x)$ is the reduced ($\text{Mü}_d(0) = 1$) d-wave superconducting order parameter dependence [150].

In the mixed phase, when CDWs and superconductivity coexist and compete (hereafter, we call this phase SCDW), the order parameter dependences $\Sigma(T)$ and $\Delta(T)$ differ from those inherent to the parent states, i.e. $\Sigma_0(T)$ and $\Delta_0(T)$, respectively [148, 154]. The resulting self-consistent set of gap equations, which determines $\Sigma(T)$ and $\Delta(T)$ for the given set of the input model parameters ($\Delta_0(0)$, $\Sigma_0(0)$—for brevity, they are denoted below as Δ_0 and Σ_0, respectively—α, and N) has the form obtained earlier [7, 148, 154, 155], which is given below for completeness

$$\int_{-\alpha}^{\alpha} I_M(\sqrt{\Sigma^2 + \Delta^2\cos^2 2\theta}, T, \Sigma_0) d\theta = 0, \tag{10}$$

$$\int_{-\alpha}^{\alpha} I_M(\sqrt{\Sigma^2 + \Delta^2\cos^2 2\theta}, T, \Delta_0\cos 2\theta)\cos^2 2\theta d\theta + \int_{\alpha}^{\Omega-\alpha} I_M(\Delta\cos 2\theta, T, \Delta_0\cos 2\theta)\cos^2 2\theta d\theta = 0. \tag{11}$$

Here,

$$I_M(\Delta, T, \Delta_0) = \int_0^\infty \left(\frac{1}{\sqrt{\xi^2+\Delta^2}} \tanh\frac{\sqrt{\xi^2+\Delta^2}}{2T} - \frac{1}{\sqrt{\xi^2+\Delta_0^2}} \right) d\xi \tag{12}$$

is the Mühlschlegel integral of the BCS theory. The angle Ω equals π for $N = 2$ and $\frac{\pi}{2}$ for $N = 4$. Because of the order parameter competition, one of the initial critical temperatures, T_{c0} or T_{s0}, is reduced to its actual value, $T_c < T_{c0}$ (with $T_s = T_{s0}$) or $T_s < T_{s0}$ (with $T_c = T_{c0}$), depending on whether $T_{c0} < T_{s0}$ or $T_{c0} > T_{s0}$, respectively. In high-T_c oxides and other known CDW superconductors, the observed

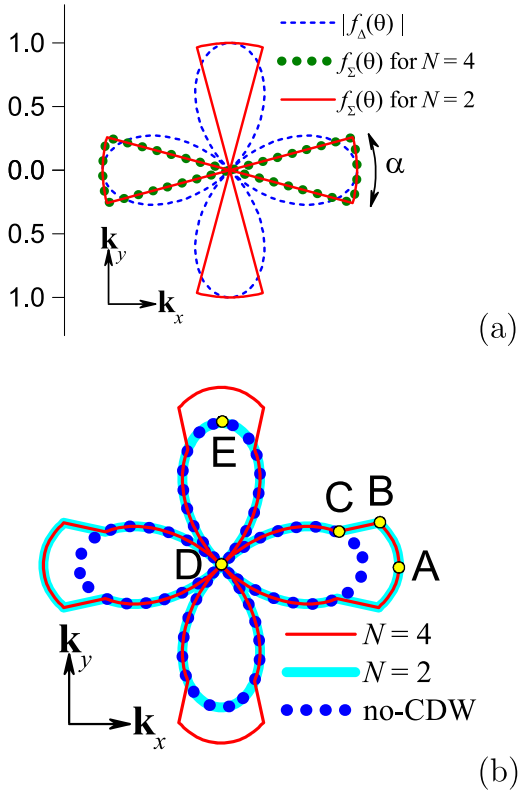

Figure 1. (a) Two-dimensional (in the *ab*-plane) angular factors for the superconducting, Δ, and CDW, Σ, order parameters of the *d*-wave superconductor with partial dielectric (CDW) gapping of its Fermi surface (FS)—dSCDW—in the momentum (**k**) space. The checkerboard ($N = 4$) and unidirectional (stripe-like, $N = 2$) CDW cases are shown. (b) Combined energy gap of the dSCDW in the **k**-space (the gap rose). The 'no-CDW' profile corresponds to the reference pure dBCS with the same superconducting order parameter as in the dSCDW. The points A to E in the gap rose mark those features in the quasiparticle spectrum that are responsible for tunnel current peculiarities. See further explanations in the text.

superconducting critical temperatures are lower than their dielectric counterparts: $T_c < T_s$ [6, 7, 9, 11, 24, 156–159].

On the dielectrized (d) FS sections, the intertwining of two order parameters leads to the emergence of a combined gap of twofold origin and no definite symmetry

$$\bar{D}(T,\theta) = \sqrt{\Sigma^2(T) + \bar{\Delta}^2(T,\theta)},$$

whereas the 'purely' superconducting gap $\left|\bar{\Delta}(T,\theta)\right|$ exists on the remaining nd part of the FS. The overall angle-dependent gap spanning the whole FS (called by us the gap rose, see figure 1) can be written in the form

$$\bar{D}(T,\theta) = \sqrt{\bar{\Sigma}^2(T,\theta) + \bar{\Delta}^2(T,\theta)}, \tag{13}$$

where

$$\bar{\Delta}(T,\theta) = \Delta(T) f_\Delta(\theta), \tag{14}$$

$$\bar{\Sigma}(T,\theta) = \Sigma(T) f_\Sigma(\theta). \tag{15}$$

Our phenomenological approach to the CDW pairing originates from and has its microscopic justification in the electron–phonon (Peierls) [4–6, 45, 160–163] and electron–hole (Coulomb, excitonic) [4–6, 24, 161, 164–166] scenarios. Both theoretical models have been extensively studied and discussed for decades [4–7, 9, 11, 161, 163]. The problem consists in their applicability to specific superconducting low-dimensional materials prone to the CDW instability, in particular, cuprates [11, 49, 154, 167–169], trichalcogenides [9, 170] and dichalcogenides [24, 34, 35, 161]. Indeed, the existence of the nested FS sections [161, 163] (or some kind of hidden nesting [171–173]) is not enough to guarantee a phase transition into the CDW state, because the divergence of the polarization operator [174] can be cancelled out if one takes into account its renormalization by many-body correlations [161, 175–177]. A similar renormalization, which is more familiar, concerns itinerant (Stoner–Wohlfarth) magnetics, where the magnetic susceptibility is enhanced by the Coulomb interaction leading to either ferromagnetic ($\mathbf{Q} = 0$) or spin-density-wave ($\mathbf{Q} \neq 0$) states [178].

As was indicated in Introduction, the very existence of CDW-PCLD distortions in cuprates is beyond any doubt. On the other hand, their origin as a consequence of the FS section nesting, as well as the development of the giant Kohn anomaly [45, 161, 174, 179], needs to be conclusively proved by further experiments. Anyway, the observed analogy [8, 24, 36, 180–182] between high-T_c oxides, on the one hand, and dichalcogenides with their huge CDWs and high T_s's, on the other hand, testify that this scenario is quite realistic. Of course, the role of electron-electron correlations may be important as well [24, 163, 176]. Nevertheless, the foregoing discussion indicates that our phenomenological model rests on strong theoretical and empiric foundations.

The mean-field approach was adopted for both order parameters. This is quite suitable for *s*-wave superconductors [183], but might be too crude for their *d*-wave counterparts because of their small coherence length ξ, not to talk about their CDW background. However, the measured temperature dependences of superconducting gaps have typical mean-field forms (in the reduced variables!), being similar to both *d*- and *s*-symmetries [7, 22, 148, 154, 184]. Furthermore, considering combined gaps in which the CDW contribution dominates (as was indicated above, since the superconducting order parameter spans over the whole FS, such gaps are always determined by the both order parameters), small observed ξ's for CDWs do not substantially distort the mean-field form of the normalized Mühlschlegel-like *T*-dependence for the dielectric order parameter. For instance, such a behavior was recently observed in tetragonal $HgBa_2CuO_{4+\delta}$ [185].

2.2. Quasiparticle currents in break junctions

In this work, we restrict the consideration to the study of quasiparticle tunneling in the *ab* plane (the set-up appropriate to BJs) between two pieces of the same oxide crystal; the latter is assumed to be a *d*-wave SCDW (dSCDW). Experimental CVCs so measured [136] differ substantially from their counterparts obtained in the '*c*-axis' experimental configuration. As is demonstrated below, the theoretical CVCs obtained

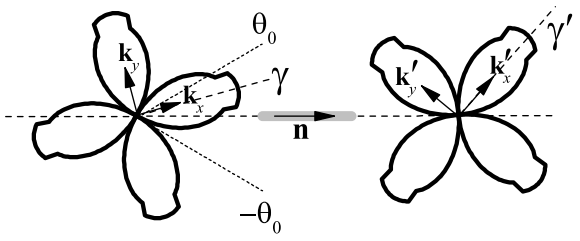

Figure 2. Two-dimensional (in the *ab*-plane) scheme of the BJ between two identical rotated pieces of dSCDW. The angle $2\theta_0$ describes the directionality cone. The vector **n** shows the direction of the current channel. The angles γ and γ' are rotational angles of the dSCDW pieces reckoned from the vector **n**. See further explanations in the text.

in the framework of our approach also differ rather strongly from the dependences calculated for the case of '*c*-axis' tunneling [83–85, 155]. It should be noted that, although BJs are most often prepared from single crystals in such a manner that the observed Josephson or quasiparticle tunneling should occur along the CuO_2 planes [137, 186, 187], the crystals can be easily (unintentionally) cleaved along the *ab* planes during the junction processing, so that there is a large probability for a *c*-axis-directed tunneling junction to be formed [139]. High-T_c-oxide BJs can also be intentionally produced to ensure tunneling along the *c*-axis with clear-cut gap-edge features [188].

To describe some of the parameters used in our model, we should consider the BJ fabrication and its consequences in some detail. A single high-T_c crystal is broken along the *c*-axis. Nevertheless, the surfaces of the pieces obtained are not atomically smooth planes, but are characterized by a very complicated rough relief: randomly arranged valleys and ridges. After the sample is broken, the both obtained pieces are moved closer to each other until the tunnel current becomes noticeable. It is most probably that the current channel emerges between a pair of points (or a few channels between a few point pairs) located across the inter-electrode gap. It is evident that the latter cannot be considered as a flat interlayer with a constant thickness. Moreover, due to the complicated relief of both junction banks, one cannot expect that the points at the current channel ends adjoined before the fracture. Therefore, the orientation of each of the high-T_c oxide pieces with respect to the relevant electrode edge can be arbitrary. Figure 2 schematically illustrates this situation. As was decribed in the previous section, the spatial orientation of each electrode can be fixed by indicating the direction of the corresponding vector $\mathbf{k}_x$. But the orientations of both 0- and V-electrodes may not coincide with those of the fracture sides, the latter playing the role of the current channel ends. Therefore, we suppose that the angles γ and γ' describing the orientation of electrodes (vectors $\mathbf{k}_x$ and $\mathbf{k}'_x$, respectively) with respect to the current channel direction (the vector **n**) may vary within a rather wide interval $-90^\circ \leqslant (\gamma, \gamma') \leqslant 90^\circ$. In the case $N = 4$, the vectors $\mathbf{k}_x$ and $\mathbf{k}_y$ in both electrodes become equivalent, and the corresponding interval of their possible orientations is $-45^\circ \leqslant (\gamma, \gamma') \leqslant 45^\circ$.

It is important to notice that, in the case of several current channels, the registered current is the sum of several (an unknown number!) current contributions with different weights. Therefore, the task of CVC interpretation becomes rather problematic taking into account the diversity of CVC profiles that are demonstrated below. That is why one of the aims of this work is to find possible components of the overall experimental CVCs. In other words, every calculated CVC corresponds to a single current channel between two identical dSCDWs differently oriented with respect to the BJ.

All those speculations concern not only the experimentally preferential tunneling [139] in the *ab*-plane. Actually, as was indicated above, the current paths lie off two dimensions. Therefore, current channels may arise not only in the *ab*-plane. As a result, the CVCs of the '*ab*'- and '*c*'-types may be superimposed, which makes the task of CVC interpretation much more difficult. A reasonable solution in this situation is to seek for CVC peculiarities that are independent of the electrode orientation.

Actually, the quasiparticle conductances of BJs descending from the same crystal batch may demonstrate a certain variety corresponding to different tunnel directions with respect to the crystal axes and some kind of gap-averaging in the lateral junction plane [86]. It seems reasonable that broken polycrystalline samples may exhibit a mixture of along-*c*-axis and in-*ab*-plane properties of $G(V)$ but with the same gap positions, as was shown, e.g. for $Bi_2Sr_2CaCuO_{8+\delta}$ [188].

In the framework of the conventional approach [189], the current $J(V)$ between a normal metal and a superconductor or between two superconductors is a functional of the products G_1G_2, where G_i means the so-called normal Green's function of the *i*th electrode. In our case, G_i denote the 'normal' Green's functions of the dSCDW. Since the electron spectrum in both BJ electrodes (the latter are two pieces of the same initial sample) is CDW-gapped, the identification as 'normal' for Green's functions is a matter of convention. Indeed, in addition to the ordinary normal Green's functions of the SCDW, which are proportional to the averages $\left\langle a^\dagger_{i,\mathbf{k},\sigma} a_{i,\mathbf{k},\sigma} \right\rangle$, one must take into account Green's function G_{ib} generated by electron–hole pairing and proportional to the average $\left\langle a^\dagger_{i,\mathbf{k},\sigma} a_{j,\mathbf{k}+\mathbf{Q},\sigma} \right\rangle$ [165, 190]. This 'normal' quantity can also be called 'anomalous', since it contains the CDW order parameter $\bar{\Sigma}(\mathbf{k}) = \Sigma_0(T) f_\Sigma(\theta) e^{i\varphi}$ as a factor, in the same way as the Gor'kov Green's function F is proportional to the factor $\bar{\Delta}(\mathbf{k})$, i.e. the superconducting order parameter [189, 191]. Hence, the function G_{ib} plays an important role in the quasiparticle tunneling both between normal and superconducting partially dielectrized CDW metals [192–194].

As was indicated above, we assume that quasiparticle tunneling proceeds in the *ab*-plane of both dSCDW electrodes (as is nominally appropriate to break-junctions [86, 109, 137, 188]). We also consider the tunneling process to be coherent and take into account tunnel directionality [143–147]. Here, the coherent character of tunneling is supported by experiments for Josephson tunneling [140–142], and both coherence and directionality turn out crucial to make the actual CVC substantially different from its counterpart in the incoherent case appropriate to the *c*-axis-directed current [85, 155].

On the basis of the adopted assumptions, the formulas for the quasiparticle tunnel current can be obtained in the conventional way [189, 191] and similarly to our earlier calculations made for other cases dealing with both *s*-wave and *d*-wave SCDWs [6, 82, 194–197]. As in the previous treatments, the phenomenological tunnel-Hamiltonian approach was used [198]. All properties of tunnel barrier were incorporated into a single constant R describing the barrier resistance in the normal state.

Since tunneling quasiparticles are confined to the *ab* plane, we include the directionality factor and the angles γ and γ' between the *a*-axes of crystalline electrodes and the vector **n** oriented perpendicularly to the junction plane. The studied BJ configuration is depicted in figure 2. Some misorientation between the BJ electrode axes was experimentally found in $YBa_2Cu_3O_{7-\delta}$ [109]. Taking into account the relevant parameters in the same manner as was done earlier when calculating the Josephson current [147] and using the same notations, we arrive at the following formula for the coherent current $J_{ab}(V)$ across the BJ:

$$J_{ab}(V,\gamma,\gamma') = \frac{1}{2\,(2\pi)\,eR}\int_{-\pi}^{\pi} d\theta \cos\theta\; W(\theta) \times \int_{-\infty}^{\infty} d\omega K(\omega,V,T)\; P(\omega,\theta-\gamma)\; P'(\omega-eV,\theta-\gamma'). \tag{16}$$

Here, e is the elementary charge. The quantity

$$K(\omega,V,T) = \tanh\frac{\omega}{2T} - \tanh\frac{\omega-eV}{2T} \tag{17}$$

is the Fermi-distribution-related factor, whereas the P functions describe electrodes. The primed quantities are associated with the electrode under the potential V (the V-electrode); the other (earthed) electrode will be referred to as 0-electrode. In particular, for the 0-electrode,

$$P(\omega,\theta) = \frac{\Theta\left(|\omega| - \bar{D}(T,\theta)\right)}{\sqrt{\omega^2 - \int \bar{D}^2(T,\theta)}} \times \left[|\omega| + \mathrm{sign}\,\omega\;\cos\varphi\;\bar{\Sigma}(T,\theta)\right], \tag{18}$$

where $\Theta(x)$ is the Heaviside step-function. The CDW phase φ is usually pinned by the junction interface and acquires a value of 0 or π (see discussion in [6, 7]), and $\bar{D}(T,\theta)$ and $\bar{\Sigma}(T,\theta)$ are the gap and CDW-order-parameter profiles on the Fermi surface described by formulas (13) and (15), respectively. For $P'(\omega-eV,\theta')$, the variable ω in formula (18) has to be changed to $\omega - eV$, and all other parameters, but T, have to be primed, i.e. associated with the V-electrode. The peculiar term in the brackets of equation (18) is generated by the electron–hole-pairing Green's function G_{ib}, discussed above. It was first applied to tunneling between Peierls insulators [199] and leads to the CVC asymmetry in *non-symmetric* junctions involving SCDWs [192, 195]. For truly symmetric junctions, such terms are present in the constituent current components, but they become mutually compensated from equations of type (16) for the tunnel currents.

The coherent character of tunneling means that the integration in the momentum space is carried out over the single angle variable θ. In the framework of the tunnel Hamiltonian method, we should summarize all current contributions between the quasiparticle states in the 0-electrode (the variable θ) and the V-electrode (the variable θ'), i.e. we should integrate over the product of two momentum spaces. The integration over θ' is reduced by introducing the function $\delta(\theta'-\theta)$.

The origin of two directionality factors $\cos\theta$ and $W(\theta)$ was discussed earlier while studying both the quasiparticle and Josephson currents [11, 145, 147, 200–207]. The discussion of this issue will be continued in the next section.

2.3. Tunnel directionality

The coefficient $\cos\theta$ in equation (16) originates from the factors $|\mathbf{v}_{g,nd}\cdot\mathbf{n}|$ and $|\mathbf{v}_{g,d}\cdot\mathbf{n}|$ (here, $\mathbf{v}_{g,nd} = \nabla\xi_{nd}$ and $\mathbf{v}_{g,d} = \nabla\xi_d$ are the quasiparticle group velocities for the corresponding FS sections [201, 202]), which are proportional to the number of electron attempts to penetrate through the barrier [208]. The multiplier $\cos\theta$ makes allowance for only the normal projection of the quasiparticle motion with respect to the tunnel junction plane while calculating the total tunnel current through the junction [205, 208, 209].

The quantity $W(\theta)$ is the barrier penetration factor [144, 209, 210], which we assume to be energy-independent, so that

$$W(\theta) \approx AY(\theta), \tag{19}$$

where the coefficient A is identical for all relevant ω's in integral (16). As a result, the factor A, can be factorized out to form, together with other pre-integral multipliers, the normal-state junction resistance, R. The factor $\cos\theta$, together with the function $Y(\theta)$ (formula (19)), makes the contribution of a tunneling quasiparticle into the total current dependent on the angle at which the quasiparticle transverses the junction. This is the so-called tunnel directionality [23, 143–147, 204].

The crucial role of the tunnel directionality, which has been perceived long ago, can be especially spectacular for the BJ tunneling. Indeed, the voltage dependences of the tunnel conductance $G(V)$, i.e. the CVCs, are often used to determine the superconducting energy gaps and pseudogaps, whatever the nature of the latter, in the junction electrodes [137, 211–213]. However, the restrictions imposed by tunnel directionality on the current formation in the BJ configuration may make the results ambiguous. Specifically, the contributions of those Fermi surface sections that fall outside the 'tunneling cone' ($|\theta| > \theta_0$, see figure 2) can be effectively 'cut off', so that the spectral peculiarities associated with the FS peculiarities located in the 'cut-off' sections will weakly (or will not at all) manifest themselves in actual CVCs. Below we will illustrate this circumstance. The exact form of the directionality function $Y(\theta)$ is not known. Therefore, we tried several of them. Expectedly, the positions of the gap-related CVC peculiarities turned out independent of the choice of $Y(\theta)$. At the same time, the CVC form can change substantially, especially if the *d*-wave node regions are involved. Since the qualitative picture remains the same for all realistic trial $Y(\theta)$ dependences with the same cut-off angle θ_0, we present hereafter the results obtained mainly for the specific $Y(\theta)$,

$$Y(\theta) \sim \begin{cases} \left(\theta_0^2 - \theta^2\right)^2 & \text{if } |\theta| \leqslant \theta_0, \\ 0 & \text{otherwise.} \end{cases} \quad (20)$$

The selected phenomenological model completely suppresses the contributions of the FS sections falling beyond the tunneling cone θ_0 to the CVC. It was done in order to make the directionality effect more pronounced. Anyway, the character of tunnel directionality [23, 143–147, 204] is satisfactorily described by simple function (20).

It is clear that, in the framework of the model concerned, the importance of certain FS sections in the CVC formation strongly depends on the orientation of the BJ electrode crystal lattices relative to the current channel. Since we consider nominally symmetric junctions between two identical dSCDWs, the common superconducting order parameter amplitude Δ_0 was chosen as the energy scale and used to present the results in the normalized dimensionless form.

3. Results of calculations and discussion

3.1. Preliminary remarks

The large number of model parameters in the problem concerned makes its complete and comprehensive analysis rather a hard task. Therefore, we confine the consideration to some parameter sets, which we believe to be illustrative enough. As was marked above, the experimental quasiparticle tunnel CVC for a BJ can be the sum of a few contributions with different weights. The results presented below undoubtedly demonstrate how diverse those contributions can be.

It is easy to see that all parameters having the dimensionality of energy (these are the both order parameters and the combined gap) for the dSCDW can be normalized by the parameter Δ_0: $\delta = \Delta/\Delta_0$, $\sigma = \Sigma/\Delta_0$. Accordingly, the 'parent' parameter set $(\Delta_0, \Sigma_0, \alpha)$ can be reduced to (σ_0, α). This normalization is all the more reasonable because the BJ electrode are pieces of the same dSCDW, and, hence, they are supposed to be described by the same parameter set $(\sigma_0 = \sigma_0', \alpha = \alpha')$. Using the parameter Δ_0, we also introduce the dimensionless bias voltage $v = eV/\Delta_0$.

More specifically, we selected the sets $\sigma_0 = (1, 1.3)$ and $\alpha = (5°, 10°, 20°)$ for the 'parent' parameters (σ_0, α) of electrodes as the reference ones (the value $\delta_0 = 1$ is implied). We chose them to illustrate the CVC behavior for the different ratios between the 'actual' order parameter magnitudes, $\delta < \sigma$ or $\delta > \sigma$. The self-consistent values of the parameters δ and σ at the zero temperature, $T = 0$ K, which govern the CVC form, are quoted in table 1 for both CDW configurations ($N = 2$ and 4). In table 1, we also quote the values of $\bar{D}$-function (13) at specific gap-rose points. The latter are specific points in the dSCDW quasiparticle spectrum and manifest themselves in the quasiparticle CVCs.

In some cases, we illustrate the influence of CDWs on a specific quasiparticle CVC by calculating the corresponding CVC for a BJ prepared from a reference pure dBCS. The latter has the same superconducting order parameter δ calculated for its dSCDW counterpart at the given temperature in the framework of the self-consistent scheme [148, 154] adopted here, but is free of CDWs ($\sigma_0 = 0$). The corresponding gap rose is depicted in figure 1 as no-CDW. We will also call such CVCs as no-CDW ones. As a rule, the CDW influence looks like a distortion of the corresponding no-CDW CVCs. However, attention should be paid to the fact that tunnel directionality makes CVCs very different from those obtained in the non-coherent scenario (independent integration over θ and θ' in the formula for the tunnel current) and neglecting tunnel directionality (the function $Y(\theta) = \text{const}$ in equation (19), and the multiplier $\cos\theta$ is put equal to unity in equation (16)). In the latter case, we obtain the CVCs shown in figure 3 [150], which will be further used for comparison.

Table 1. Self-consistent values of order parameters and the values of $\bar{D}$-function (13) at characteristic gap-rose points (see figure 1) for reference problem parameter sets[a].

	$N = 2$			$N = 4$		
	α			α		
	5°	10°	20°	5°	10°	20°
	$\sigma_0 = 1$					
δ	0.999	0.994	0.950	0.998	0.984	0.778
σ	0.106	0.225	0.485	0.113	0.262	0.696
A	1.005	1.019	1.067	1.005	1.019	1.045
B	0.989	0.961	0.875	0.989	0.962	0.917
C	0.984	0.934	0.728	0.983	0.925	0.596
D	0	0	0	0	0	0
E	0.999	0.994	0.950	—	—	—
	$\sigma_0 = 1.3$					
δ	0.967	0.926	0.812	0.927	.810	0.348
σ	0.873	0.930	1.062	0.915	1.029	1.259
A	1.303	1.313	1.337	1.303	1.310	1.306
B	1.292	1.274	1.231	1.293	1.280	1.287
C	0.952	0.870	0.622	0.913	0.761	0.266
D	0	0	0	0	0	0
E	0.967	0.926	0.812	—	—	—

[a] See notations in the text.

For convenience, the temperature was normalized by the real superconducting critical temperature T_c rather than its parent value T_{c0} (see discussion in section 2.1), i.e. $t = T/T_c$. The difficulty consists in that T_c has not such a simple relationship with the actual order parameters as its counterpart T_{c0} has with the parent ones.

The quasiparticle tunnel current J (see equation (16)) in the dimensionless form looks like $j = \frac{1}{eR\Delta_0}J$. We are interested in the tunnel conductance $G = \mathrm{d}J/\mathrm{d}V$ and its dimensionless analog $g = R\,\mathrm{d}J/\mathrm{d}V$ that equals $\mathrm{d}j/\mathrm{d}v$ (see the definition of v above). As was done in our previous works [155, 197], we simulated the routine of finding g by calculating the finite difference

$$g(v) \approx \frac{1}{2\,\Delta v}\left[j(v + \Delta v) - j(v - \Delta v)\right]. \quad (21)$$

The differentiation step was put equal to $\Delta v = 0.001$.

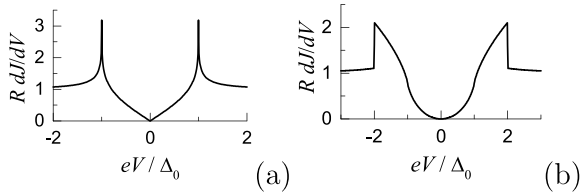

Figure 3. Dimensionless quasiparticle CVCs $G(V) = R\mathrm{d}J/\mathrm{d}V$ calculated in the basic model of tunneling between dBCSs [150], i.e. neglecting directionality effects, for the temperature $T = 0$. Here, J is quasiparticle the tunnel current, and R the normal-state resistance of the junction. Panel (a) describes a non-symmetric junction between a d-wave superconductor and a normal metal, and panel (b) a symmetric junction between two identical dBCSs. In the framework of Won–Maki model [150], those CVCs are universal and do not depend on the electrode orientation. See further explanations in the text.

The basic value of the directionality-cone opening θ_0 was selected to be rather narrow, $\theta_0 = 10°$, in order to make the directionality effects more pronounced. One should pay attention that the parameter θ_0 determines the θ-interval beyond which all allowed current contributions are strictly nullified. At the same time, the bell-shaped profile of $Y(\theta)$ additionally suppresses contributions with θ-values located near the interval ends. The half-width of the peak equals about 10°, so that the directionality angle of 'effective' tunneling equals about 5° in this case.

The dielectric order parameter phase φ is considered equal to π. It is done for definiteness, although the intrinsic origin and the sign of the phase φ is not known. However, a possible loss of symmetry with respect to the sign of V in non-symmetric junctions with one normal or superconducting metallic electrode, gapped by CDWs, is beyond any doubt. It was observed in a number of high-T_c oxides by STM measurements [214–219].

3.2. Zero temperature

Typical BJ experiments are carried out at the temperature $T = 4.2$ K, which is much lower than T_c's for the majority of high-T_c oxides. Temperature-induced effects (smearing) do not manifest themselves near the absolute zero, so it seems reasonable first to calculate quasiparticle tunnel CVCs for $T = 0$ K.

3.2.1. Directionality. To emphasize the role of directionality, it is instructive to present a series of $G(V)$ dependences for different angles θ_0, which in essence comprises the influence of the effective current channel length distance L between BJ electrodes, the relationship between θ_0 and L being far from non-linear [144, 147, 200]. Let us first consider the most trivial case when the electrodes (their active regions at the current channel ends) are not rotated with respect to each other. The CVC for the electrode orientation $\gamma = \gamma' = 0°$ with respect to the current channel is demonstrated in figure 4(a). Here, the parent CDWs and superconductivity were taken to be equally strong ($\sigma_0 = 1$). The other parameters are $N = 4$ and $\alpha = 10°$

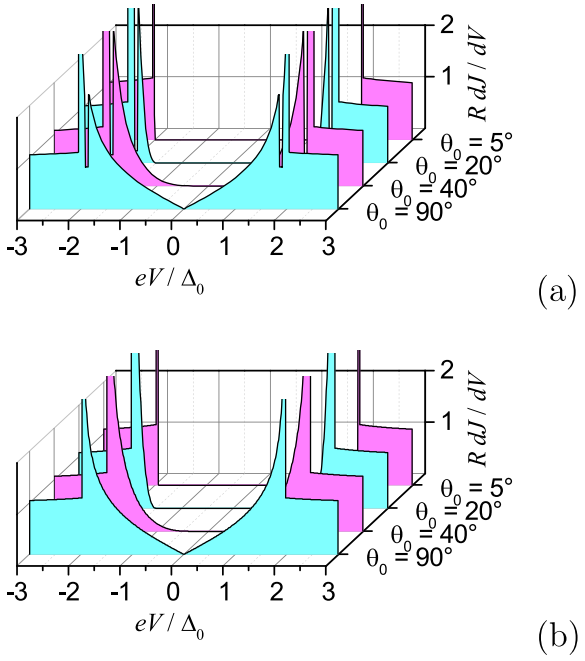

Figure 4. (a) CVCs and (b) their no-CDW counterparts calculated for $T = 0$, $N = 4$, $\alpha = 10°$, $\sigma_0 = 1$, $\gamma = \gamma' = 0°$, and various θ_0's.

(see the relevant parameters of gap rose in table 1. Figure 4(b) is the no-CDW variant of panel (a).

Attention is attracted by the fact that the CVC character changes from the s-wave one at strong directionality (relatively large inter-electrode distances corresponding to small θ_0's) to those similar (only similar!) to a V-like CVC for a non-symmetric tunnel junction between a dBCS and a normal metal (see figure 3(a)), although now the junction is perfectly symmetrical including the electrode orientations. Therefore, any attempt to make a definite conclusion on the actual order parameter symmetry from the apparent BJ quasiparticle CVCs seems to be not compelling. At the same time, the comparison of both panels makes the CDW influence on CVCs evident. For the selected CDW parameter set, CDW gapping leads to the steep fall and subsequent recovery of the smooth superconductivity-driven $G(V)$. This conclusion is confirmed by two facts. Firstly, this effect is absent a small θ_0, since in this case only a smooth arc around the apex of the gap rose lobe takes part in the current formation, whereas the section BC (see figure 1) is left beyond the tunnel cone θ_0. Secondly, the 'eV-width' of this peculiarity, if the latter takes place, is driven by the difference $\bar{D}(\mathrm{B}) - \bar{D}(\mathrm{C})$ between the combined gap values (see equation (13)) at the indicated points, i.e. by the value of the parameter σ.

However, another CDW effect on quasiparticle CVCs remained hidden in figure 4 due to the correlated ($\gamma = \gamma'$) electrode orientations. Let one of the crystalline electrodes, for instance, the V-one, be rotated in such a way that $\gamma' = 45°$. The CVC profiles change their form drastically, as is displayed in figure 5. At small θ_0's, the CVCs are apparently s-wave ones and imitating those for *non-symmetric* junctions. Indeed, the V-electrode is gapless inside the θ_0-opening. As a consequence, the separation between the coherent peaks is 2Δ,

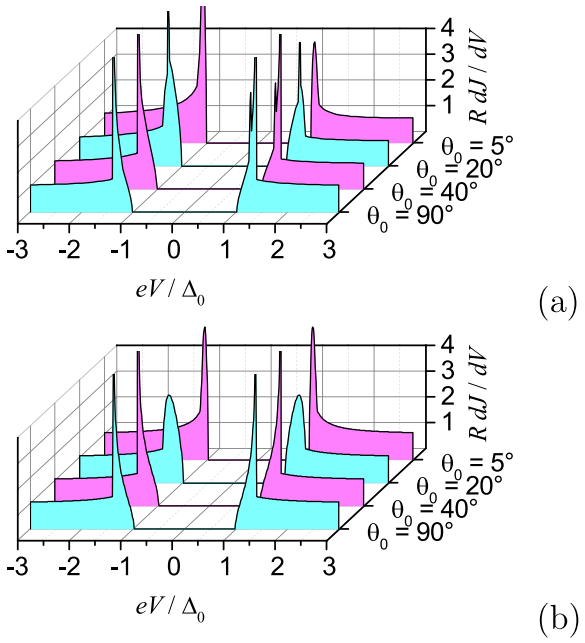

Figure 5. The same as in figure 4, but for $\gamma' = 45°$.

appropriate to the S-I-N (S, I, and N stand for a superconductor, an insulator, and a normal metal, respectively) configuration, instead of the 4Δ, as it should be in the truly symmetric S-I-S junctions. When θ_0 grows, this feature survives up to $\theta_0 = 90°$. On the other hand, the peaks are shifted towards larger biases, and the CVC form is distorted tending to the *d*-wave pattern. The apparently S-I-N conductances were found, e.g., in BJ experiments for $La_{1.85}Sr_{0.15}CuO_4$ single crystals broken perpendicular to the tetragonal (1 1 0) direction [220].

The comparison of the CDW-containing (panel (a)) and 'no-CDW' (panel (b)) CVCs demonstrates again that the 'gap-like' CDW-induced density-of-states gapping in the CVCs appear only when the BC section in the gap rose becomes included into the tunneling cone. But what is much more spectacular is the loss of CVC symmetry with respect to the bias voltage sign. It is so, because the nominal S-I-S symmetry is broken by the V-electrode rotation. As a consequence, the current terms originating from the electron–hole pairing and proportional to $\bar{\Sigma}(\mathbf{k}) = \Sigma_0(T) f_\Sigma(\theta) e^{i\varphi}$ do not mutually compensate each other for both *V* polarities. Being summed up with other current, *J*, components that are inherently antisymmetric with respect to the bias voltage sign, they violate the overall CVC symmetry, as was found in BJ studies [109, 138, 220–225]. Note that the symmetry violation is observed for all θ_0-values in this experimental setup. Hence, the proper account of tunnel directionality is an important factor for the adequate interpretation of quasiparticle CVCs.

In addition to the conjectures presented earlier [226], the manifestations of the anomalous term in the rotated ($\gamma \neq \gamma'$) configurations comprise another reason, why CDWs can lead to the CVC symmetry breaking in the formally symmetric setup. We emphasize that in the absence of CDWs the curves $G(V)$ for the symmetric junctions are symmetric, *irrespective of how the electrodes are relatively oriented*. Thus, the asymmetry in the dependences $G(V)$ for non-symmetric junctions

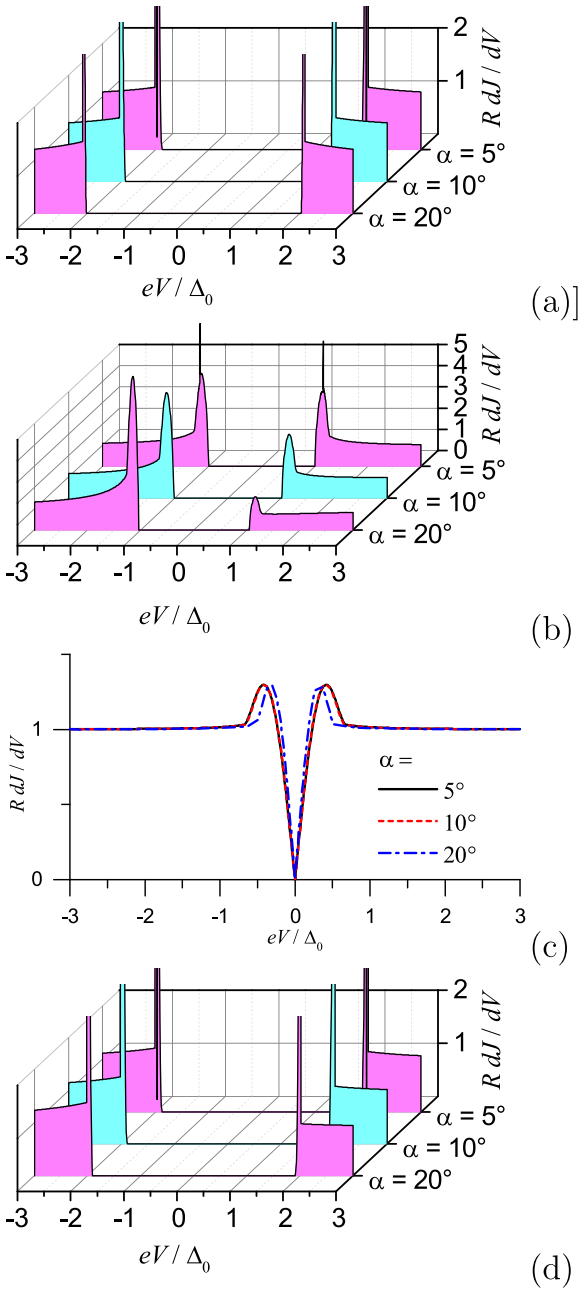

Figure 6. CVCs calculated for $T = 0$, $N = 4$, $\theta_0 = 10°$, $\sigma_0 = 1$, and various α's and for electrode orientations (a) $\gamma = \gamma' = 0°$, (b)$\gamma = 0°$ and $\gamma' = 45°$, and (c) $\gamma = \gamma' = 45°$. Panel d corresponds to $N = 2$, $\theta_0 = 10°$, $\sigma_0 = 1$, $\gamma = 0°$, and $\gamma' = 90°$.

between superconductors, in which the electron spectrum is suspected to be unstable, can be considered as a smoking gun of the inherent CDWs, especially in the case when the energy gaps cannot be unequivocally attributed. Since the role of the directionality became clear from the calculations presented above, we shall fix θ_0 at a reasonable value of 10° throughout the remaining part of the paper.

3.2.2. Electrode parameters. Let us first consider the influence of the CDW-sector width α on the $G(V)$ dependence. Figure 6(a) demonstrates this dependence for $N = 4$, $\sigma_0 = 1$, the gap-rose orientation $\gamma = \gamma' = 0°$ (the antinode-to-antinode

orientation), and various α's. In the case $\alpha = 20°$, the gaps on the active (giving a significant contribution to the current) FS areas in both electrodes are smooth and do not contain any CDW-induced peculiarities. Moreover, since $\theta_0 = 10°$ is rather small, those areas successfully mimic the sections of an isotropic *s*-wave SCDW. Furthermore, due to the coherent tunneling and the identical orientation of the gap roses with respect to the current channel, the Σ phase does not manifest itself, and the CVC is symmetrical with respect to the bias voltage sign, as was explained in section 3.2.1. As a result, the corresponding current–voltage characteristics strongly resembles CVCs typical of tunnel junctions between ordinary *s*-wave superconductors. The same situation takes place for $\alpha = 10°$. The smaller degree of FS dielectrization by CDWs results in different values of 'actual' δ and σ (they are indicated in section 3.1) than in the $\alpha = 20°$- case. The distinctive CVC points become shifted, but the CVC as a whole preserves its profile. At $\alpha = 5°$, the BC sections of the gap rose enter the tunnel cone and lead to additional peculiarities (jumps). This singularity manifests itself in the appearance of a CVC fine structure, but the CVC as a whole remains symmetric. This singularity is narrow in the case concerned, because the difference $\bar{D}(\mathrm{B}) - \bar{D}(\mathrm{C})$ is small (see table 1).

Similarly to what was considered in section 3.2.1, different electrode orientations with respect to the current channel together with coherent tunneling violate the CVC symmetry. Figure 6(b) demonstrates tunnel CVCs for the same electrodes as in panel (a), but their gap roses are differently oriented ($\gamma = 0°$, $\gamma' = 45°$, the antinode-to-node configuration). Again, irrespective of α, non-symmetric components of the tunnel current do not compensate one another, and the final CVC acquires a *non-symmetric* form. These results demonstrate once more that the CVC asymmetry in the symmetric junctions can be considered as evidence of CDWs even if the CDW-driven additional coherent peaks and their superconducting counterparts merge together. The active FS area of the 0-electrode mimics the *s*-wave superconductor gap, whereas that of the V-electrode contains a node and can be approximately considered as belonging to a normal metal. As a result, the final CVCs have some common features with CVCs for the tunnel junction *s*-wave superconductor-normal metal. Again, a fine structure of CVC emerges when the active FS section of 0-electrode includes the CDW-induced gap singularity.

Figure 6(c) demonstrates the same CVC set for the same electrodes, but in this case the latter have the symmetric orientations $\gamma = \gamma' = 45°$ (the node-to-node configuration). As a result, the exhibited CVCs are symmetric again. Even at $\alpha = 20°$, the sections of electrode gap roses in the tunnel cones do not include singular points. Therefore, the corresponding CVCs remain smooth, except for the zero-bias voltage region. The CVCs for $\alpha = 5°$and $10°$ almost coincide, because the values of δ and σ in the both cases are almost identical (see table 1). (That is why the $\alpha = 5°$- and $\alpha = 10°$-CVCs in panels (a) and (b) are also almost identical, with an accuracy to the fine structure in the $\alpha = 5°$-case.) For $\alpha = 20°$, the δ- and σ-values changes enough (table 1) for the corresponding CVCs to be distinguishable from their $\alpha = 5°$- and $\alpha = 10°$-counterparts.

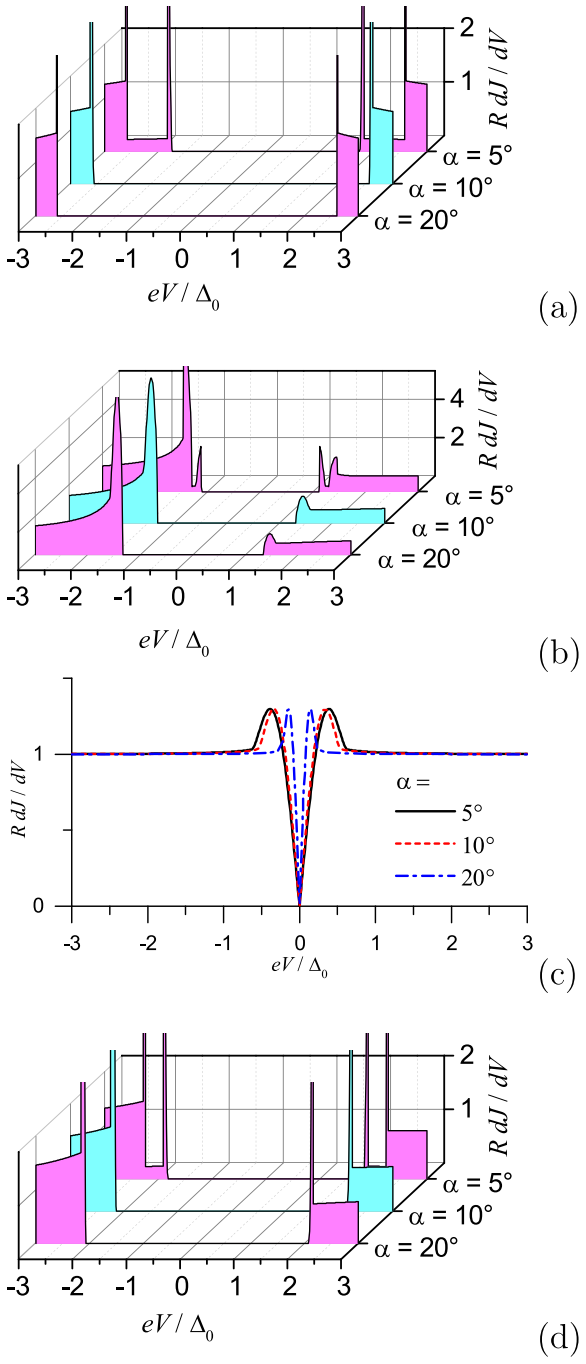

Figure 7. The same as in figure 6, but for $\sigma_0 = 1.3$.

In the case of the stripe CDW configuration ($N = 2$), the δ- and σ-values only slightly differ from their values at $N = 4$ for every α (see the data in table 1). But the form of the gap rose is quite different: it includes two partially dielectrized lobes instead of four (see figure 1). Provided the given parameter $\theta_0 = 10°$, the results for electrode orientations, which were analyzed above (figures 6(a)–(c)), will be almost the same. But for the unidirectional CDWs ($N = 2$), there is also a case that cannot be realized in the checkerboard ($N = 4$) configuration. This is the combination $\gamma = 0°$ and $\gamma' = 90°$. Then, the both gap roses 'look at each other', but the 0-gap rose contributes via its dielectrized lobe, whereas the V-gap lobe via the nondielectrized one. Therefore, the Σ phase φ

of only 0-electrode enters the calculations. As a result (figure 6(d)), the final CVCs look very similar to those depicted in figure 6(a), but they are non-symmetric. The CVC non-symmetricity gradually disappears together with the reduction of the FS dielectrization degree characterized by the parameter α. Again, when the gap on the active FS part of 0-electrode contains a singularity, the CVC peak splits.

Figure 7 demonstrates the same plots as in figure 6, but for $\sigma_0 = 1.3$. Here, the actual σ-values in each case are larger than in the case with $\sigma_0 = 1$ (see table 1), and the influence of CDWs becomes more pronounced. For this reason, the singularities in all panels are more separated and better distinguishable. In particular, for the case $\alpha = 5°$, it is instructive to compare a rather complicated construction created by two overlapping peaks in figure 6(b) and well-resolved peak pairs with a clear asymmetry with respect to the bias voltage sign in figure 7(b).

Another point concerns the relation between the spatial inhomogeneity of electrodes, including their nonstoichiometry, and the possibility to observe the predicted CVC features. In particular, the width of the cutout with abrupt edges (it will be recalled that this feature is associated with the CDW-induced discontinuity BC in the gap-rose, see figure 1(b)) is determined by the energy distance between points B and C in the gap rose. As one can see from table 1, at $\sigma_0 = 1$, this distance is very short, so that the indicated feature will be effectively smoothed out in the inhomogeneous case. At the same time, for larger σ_0's, this distance becomes rather conspicuous, and we may hope that the feature concerned will manifest itself.

It is no wonder that the CVC dependences on the FS dielectrization parameter α are similar to the dependences on the tunnel directionality cone θ_0 (see section 3.2.1). Indeed, the influence of those two angles can be, to some extent, regarded as mutually reverse. Namely, if we select a certain intermediate θ_0-value, by changing the parameter α we can either include the FS section BC (see figure 1) into the tunnel cone or leave it outside. And vice versa, the same effect can be obtained at a fixed α by varying θ_0. Of course, specific CVCs will be numerically different, but the qualitative character of corresponding changes will survive.

The dimensionless parent CDW gap σ_0 is another important parameter describing the relative strength of the electron–hole pairing (the parent d-wave Cooper pairing strength being the reference value). As is seen from the results depicted in figure 8(a) and calculated for the configuration $N = 4$, $\theta_0 = 10°$, $\gamma = 0°$, $\gamma' = 0°$, the growth of σ_0 results mainly in the widening of the gap region. Therefore, in this case of strong directionality (large enough electrode separations), it is impossible to detect CDWs in CVCs of such break junctions. The situation changes drastically for the weakened directionality, e.g. for $\theta_0 = 20°$ being twice the parameter $\alpha = 10°$, as comes about from the results displayed in figure 8(b). Here, the directionality cone almost completely encloses the two active rose-gap lobes with all their singular points (see figure 1). As a consequence, the CVCs exhibit double-peak structures heavily dependent on σ_0. Therefore, break junctions with small effective inter-electrode distances can serve as a probe of the electron–hole pairing strength.

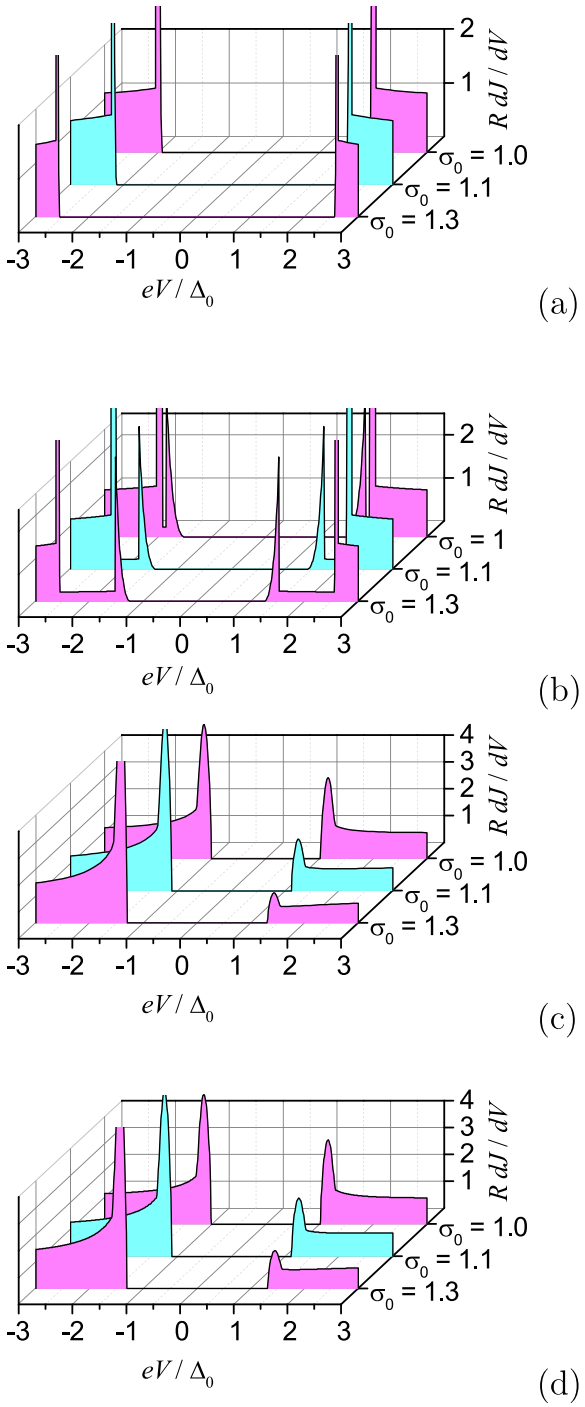

Figure 8. CVCs for the parameter sets (a) $N = 4$, $\theta_0 = 10°$, $\alpha = 10°$, $\gamma = \gamma' = 0°$; (b) $N = 4$, $\theta_0 = 20°$, $\alpha = 10°$, $\gamma = \gamma' = 0°$; (c) $N = 4$, $\theta_0 = 10°$, $\alpha = 10°$, $\gamma = 0°$, $\gamma' = 45°$; and (d) $N = 2$, $\theta_0 = 10°$, $\alpha = 10°$, $\gamma = 0°$, $\gamma' = 45°$; and for various σ_0's. $T = 0$.

The CVCs in the BJ configuration $N = 4$, $\theta_0 = 10°$, $\gamma = 0°$, $\gamma' = 45°$ is quite another matter. Although the directionality is strong and the double-peak structure is absent, the peak asymmetry induced by the CDWs is very pronounced, as can be inferred from figure 8(c). This trend survives, although being slightly reduced, for the unidirectional CDW, which is

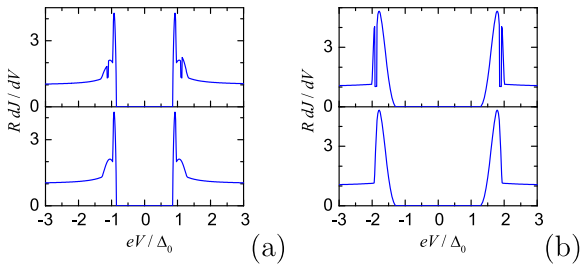

Figure 9. CVCs for BJs involving a dCDWS (upper subpanel) and its no-CDW counterpart (a pure dBCS, lower subpanel). Parameters: $T = 0$, $N = 4$, $\theta_0 = 10°$, $\alpha = 10°$, $\sigma_0 = 1$, $\gamma = 45°$ (a) and 15° (b), $\gamma' = 15°$.

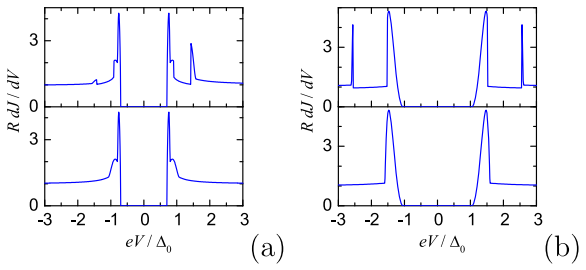

Figure 10. The same as in figure 9, but for $\sigma_0 = 1.3$.

shown in figure 8(d) for the configuration $N = 2$, $\theta_0 = 10°$, $\gamma = 0°$, $\gamma' = 45°$.

It should be noted again that the coherence-peak splitting caused by CDWS can easily be overlooked if the electron–hole pairing is weak (σ_0 is small enough). Then, a moderate disorder or an electrode surface roughness can smear the split peaks and fill the gap between them. However, the splitting effect becomes robust against impurity and surface electron scattering when the CDW influence becomes much stronger, e.g. for $\sigma_0 \geqslant 1.1$, as can be seen from figure 8(b).

3.2.3. Electrode rotation. Probably, the angular dependences of the conductances $G(V)$, i.e. the CVC dependences on the electrode rotation angles γ and γ', are the most interesting of our results. It is so because the striking diversity of experimental break-junction CVCs for cuprates probably originates from the varying configurations created by the crystal fracture. From the results presented in the previous sections, one can get an idea how diversified the quasiparticle CVCs are even if the electrodes are rotated with respect to the current channel by angles multiple of 45°. As a result, the curves $G(V)$ for arbitrarily non-symmetric configurations, when either one of the angles γ and γ' or both of them are not equal to 0° or 45°, become very involved. Before making a presentation of the corresponding dependences, it is instructive to make a comparison of CVCs for the SCDW junctions and purely superconducting ones for a selected set of parameters and rotations not being multiples of 45°.

First, let us consider CVCs for the configuration $N = 4$, $\gamma = 45°$, $\gamma' = 15°$, and $\sigma_0 = 1$ (the upper plot in figure 9(a)). It is clear that, in the framework of our approach, all *three* distinct coherent peaks (for each bias voltage polarity), which are apparent in the conductance $G(V)$, are generated by the removal of quasiparticle states from *two* energy gaps $\left|\bar{\Delta}(T,\theta)\right|$ and $\bar{D}(T,\theta)$ in the electron spectrum. Moreover, the small but conspicuous asymmetry of the peak structure confirms that the CDWs do affect the electron density of states. It is, however, not clear (i) why the number of peaks does not coincide with the number of gaps? (ii) Which peak is predominately driven by the superconducting gap? And (iii) which peak is the result of the combined action of two order parameters?

To obtain the answers, the no-CDW dependence $G(V)$ was calculated for the same geometry (the lower plot in figure 9(a)). The superconducting coherent peaks seem to become the same as in the upper plot. However, the results turned out counterintuitive. Specifically, a two-peak pattern appears without invoking any CDW! The absence of the CDW is clearly recognized, because the asymmetry of the curve displayed in the upper subpanel of figure 9(a) and appropriate to the SCDW disappears in the bottom subpanel.

Actually, the superconducting coherent peak splits due to the directionality of tunneling between the pieces of *d*-wave superconductor. Indeed, for the V-electrode gap rose inclined at the angle $\gamma' = 15°$ and the small opening $\theta_0 = 10°$, the passage of quasiparticles from the left to the right is different for two lobes of the V-electrode. At the same time, the 0-electrode is almost turned off the game by its 45°-rotation, so that the CVC looks like that for an S-I-N junction. As a consequence, two distinct maxima appear in the integrated product of the gapped densities of states contained in equation (16).

Now, when the CDWs come into play (the upper plot in figure 9(a)), two Σ-sectors enhance the gapping at the d FS sections. In the absence of superconductivity, a peak should appear at $eV = \Sigma_0(T)$ outside a partial dielectric gap in the conductance $G(V)$ for non-symmetric junctions, whereas in the symmetric junctions, this peak should be observed at $eV = |\Sigma_0(T)|$, as well as additional jumps at $|eV| = 2\Sigma_0(T)$ [193]. When both order parameters act in synergy in the configuration concerned, the Σ-related gapping at $|eV| = \Sigma_0(T)$ exists for both *V*-polarities, but no Σ-related features emerge in the $eV = 2\Sigma_0(T)$ neighborhood. The amplitudes of the CDW-related peaks are not equal for positive and negative *V* because, as was indicated above, the junction is actually non-symmetric. Since the parameter $\sigma_0 = 1$, an additional CDW feature emerges inside the split superconducting coherent peak.

To confirm our speculations, we calculated CVCs for the same set of parameters as in figure 9(a), but for the gap roses equally tilted in both electrodes: $\gamma = \gamma' = 15°$ (figure 9(b)). In the no-CDW case, the simultaneous correlated 15°-rotations of both crystal pieces ensures the S-I-S character of the CVC (the bottom subpanel in figure 9(b)). Moreover, the conductance $G(V)$ is symmetric. Contrary to what is inherent to the configuration $\gamma = 45°$, $\gamma' = 15°$, the superconducting coherent peaks are not split because the relevant gapping is complete for $\gamma = 15°$, $\gamma' = 15°$, and $\theta_0 = 10°$. Therefore, for planar BJs, purely superconducting CVCs may be split or not, depending on the rotations of fractured samples. If the CDWs are present, each of the single superconducting peaks is split, as in the configuration $\gamma = 45°$, $\gamma' = 15°$. At the same time, the dependence $G(V)$ remains practically symmetric.

If the strength of the parent electron–hole pairing becomes substantially larger than that for the *d*-wave Cooper pairing, the CVCs for dSCDWs should change their form. Indeed, in figure 10(a), the dependences $G(V)$ are shown for the same parameter set as in figure 9(a), but for $\sigma_0 = 1.3$. It is readily seen that the reference no-CDW curve (the bottom subpanel) calculated in the same manner as its counterpart for $\sigma_0 = 1$, is qualitatively the same as the curve in the bottom subpanel of 9(a). In particular, the superconducting peak is split. This splitting remains almost intact in the SCDW phase, since the peaks corresponding to the combined gap (13) lie outside the superconducting-gap region. The dielectric gapping is wide, and the peak in the positive-voltage branch is high. However, due to the configuration asymmetry, its partner in the negative-voltage branch is suppressed by the interference between the terms corresponding to the conventional Green's functions and the anomalous 'interband' ones, G_{ib}, as is seen in the upper subpanel of figure 10(a).

In the tilted symmetric configuration with $\gamma = \gamma' = 15°$ and $\sigma_0 = 1.3$, the CVCs of which is demonstrated in figure 10(b), the CDW-driven peaks are shown to be well outside the superconducting-gap region similarly to those for $\gamma = 45°$ and $\gamma' = 15°$. However, the CVCs are symmetric for the same reason as in figure 9(b).

Knowing the origin of the CVC features for the BJ tunneling in the *ab*-plane, we can present the overall panorama of the angular dependences for arbitrary configurations created after the sample fracture. Let us start from the checkerboard CDWs ($N = 4$). The dependences on the rotation angle γ' of the V-electrode are shown for different rotation angle values γ of the 0-electrode in figure 11. The CDW parameters were $\sigma_0 = 1$ and $\alpha = 10°$ for all figures. One can see a large variety of CVCs, being apparently *d*-wave or *s*-wave like. Different CVCs are formed under the decisive influence of the directionality effects. The latter select certain combinations of the *d*-wave lobes, which determine the tunneling peculiarities. The intertwining of the electron–hole and Cooper pairing leads to the multiple-peak structures. Since each BJ configuration obtained by the fracture is unpredictable, the resulting CVCs differ substantially. Only the totality of experiments can represent the full picture.

The results for the nematic phase [13, 78], when CDWs are unidirectional ($N = 2$), are depicted in figure 12 for the same set of parent parameters, as in figure 11, but other angles γ's. The conductances are very striking similarly to the checkerboard case. However, the peak appearance is quite different for both types of CDW structures. Since, both checkerboard and unidirectional CDWs can be found in the same materials [78, 154, 227], the number of possible CVC patterns increases.

3.3. Finite temperatures

In section 3.2, we presented results obtained for zero temperature. Nevertheless, the temperature evolution of the differential tunnel conductances $G(V)$ is very important as well, being an additional way to detect CDWs both below and above T_c [107, 137, 219, 228–230].

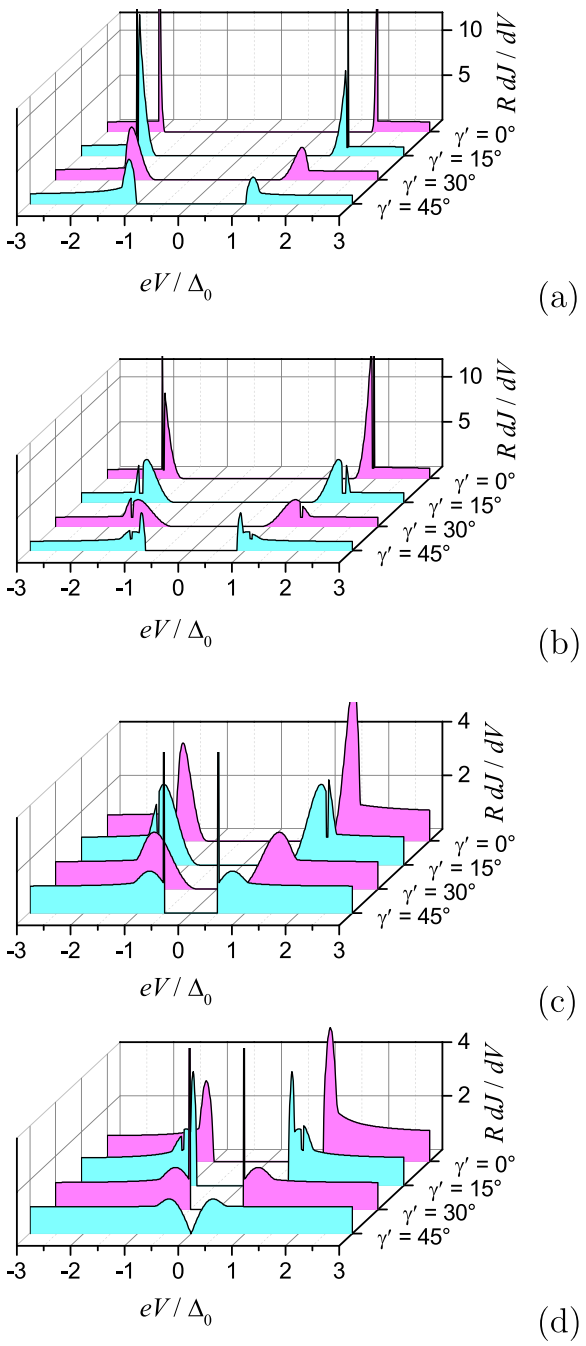

Figure 11. CVCs for $\gamma = 0°$, 15°, 30°,and 45° (panels a to d, respectively) and various γ''s. The other parameters are $T = 0$, $N = 4$, $\theta_0 = 10°$, $\alpha = 10°$, and $\sigma_0 = 1$.

The T-evolution of $G(V)$ is displayed in figure 13(a) for $N = 4$, $\sigma_0 = 1$, $\alpha = 10°$, $\theta_0 = 10°$, $\gamma = 0°$, and $\gamma' = 0°$. The parameter $t = T/T_c$ denotes the dimensionless temperature. From figure 13(a), it is readily seen that the *s*-wave-like symmetric CVC (high directionality!), which is formed by the both order parameters Δ and Σ, gradually loses the predominately superconducting coherent peaks with increasing T. At $T = T_c$, the singularities at $|eV| = \Sigma(T)$ are already suppressed by the finite T, while the others at $|eV| = 2\Sigma(T)$ survive, the both being inherent to partially gapped CDW metals [193]. For $T > T_c$, the CDW traces smoothly die out. The strong logarithmic singularity at $eV = 0$, which is shown to increase with

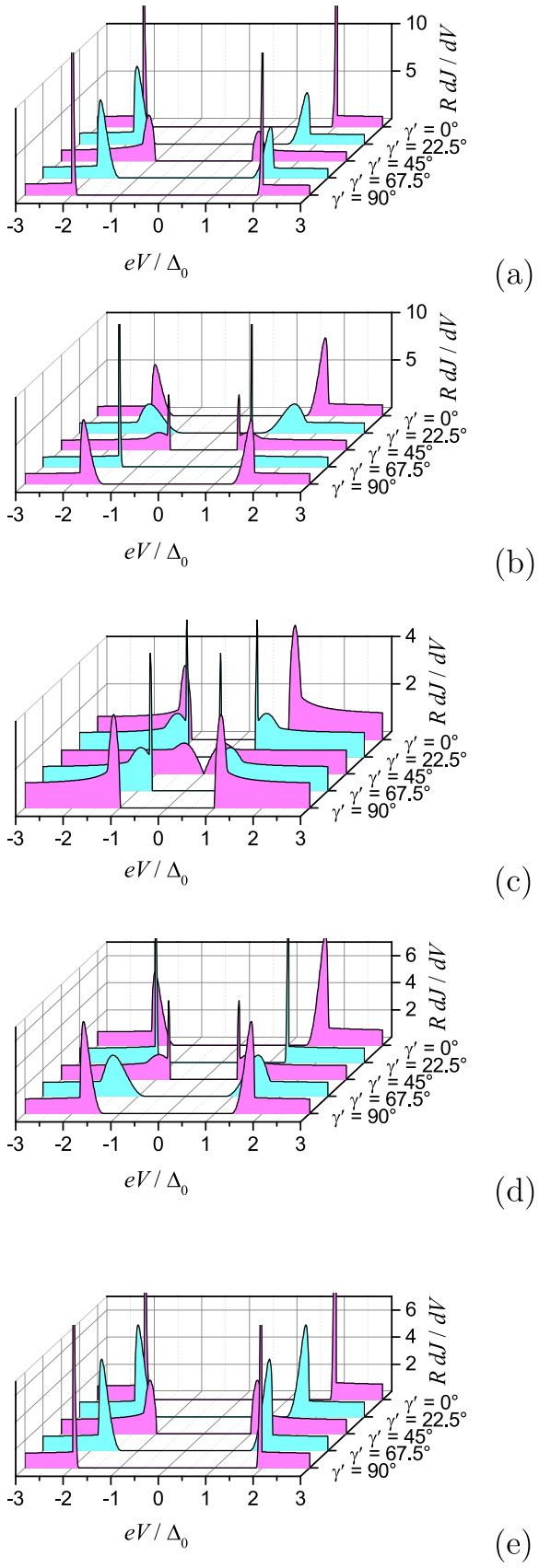

Figure 12. The same as in figure 11, but for $N = 2$ and $\gamma = 0°$, 22.5°, 45°, 67.5°, and 90° (panels (a)–(e), respectively).

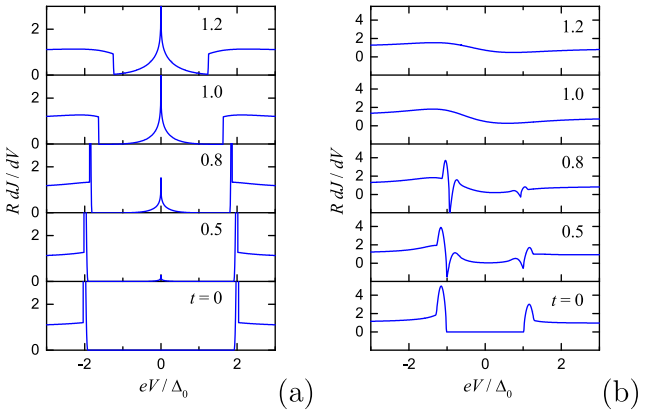

Figure 13. T-evolution of CVCs for BJs involving dCDWS with $N = 4$, $\theta_0 = 10°$, $\alpha = 10°$, $\sigma_0 = 1$, $\gamma = 0°$, and $\gamma' = 0°$ (a) and 45° (b). Here, $t = T/T_c$, and T_c is the actual critical temperature for the dCDWS concerned.

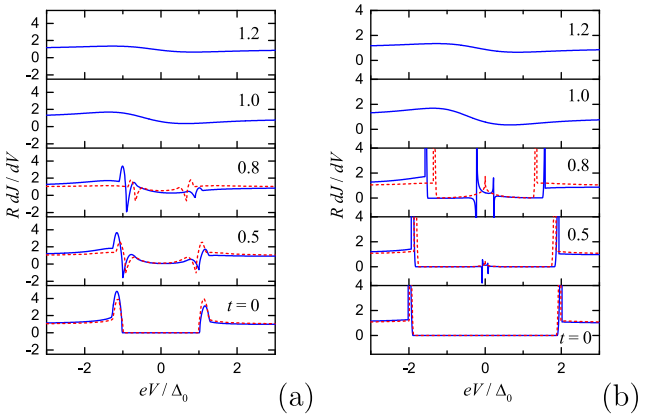

Figure 14. T-evolution of CVCs for BJs involving dCDWS (solid curves) and their no-CDW counterparts (dashed curves) for $N = 2$, $\theta_0 = 10°$, $\alpha = 10°$, $\sigma_0 = 1$, $\gamma = 0°$, and $\gamma' = 45°$ (a) and 90° (b). See further explanations in the text.

T, is appropriate to superconducting s-wave superconductors [189] as well as to partially gapped normal CDW metals. However, it is clear from figure 13(a) that this singularity also disappears for high enough t (see the upper subpanel).

If the γ' value is chosen to be 45°, the CVCs change drastically, as is demonstrated in figure 13(b). The non-symmetric $G(V)$ acquire new peculiarities, associated with the enhanced tunneling of thermally excited quasiparticles with energies equal to the difference of involved gaps. Note, that new singularities at one bias-voltage polarity look like deep negative minima, being a precursor of a possible instability and a manifestation of the CVC nonlinearity. Similar features, which had been observed in various tunnel junctions involving high-T_c oxides [231, 232], were later discussed in some detail [197]. All distinct features driven by the involved energy gaps disappear above T_c, which leaves an anomalous CDW background distorting the normal metal Ohmic conductance [193]. Negative differential conductances were also observed

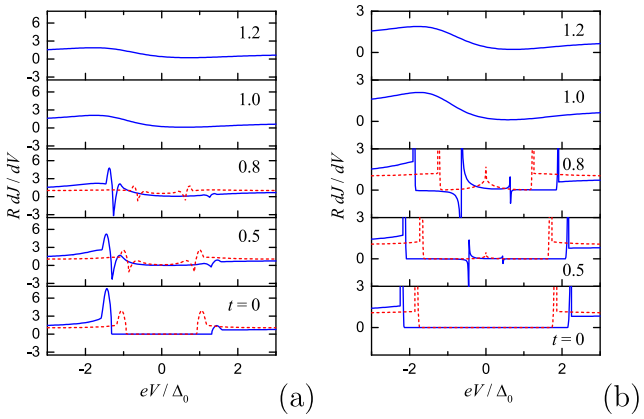

Figure 15. The same as in figure 14, but for $\sigma_0 = 1.3$.

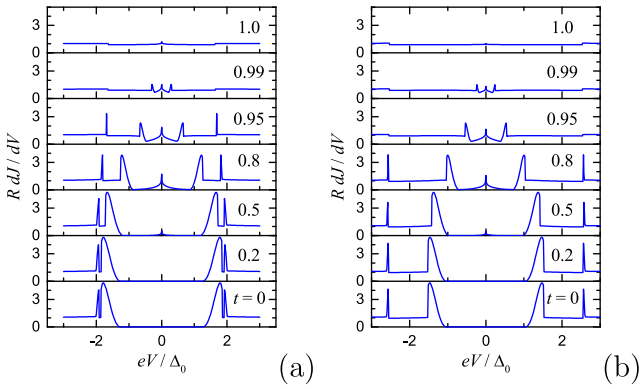

Figure 16. *T*-evolution of CVCs for BJs involving dCDWS with $N = 4$, $\theta_0 = 10°$, $\alpha = 10°$, $\gamma = \gamma' = 15°$, and $\sigma_0 = 1$ (a) and 1.3 (b).

recently at finite T in the organic Peierls insulator TTF-TCNQ [233].

In the dSCDWs with $N = 2$, i.e. in the case of unidirectional CDWs, CVCs for the symmetric, $\gamma = \gamma' = 0°$, configuration are almost the same as in the checkerboard case ($N = 4$). Hence, we considered different rotation-angle combinations. In figure 14(a), the conductances $G(V)$ are represented for $N = 2$, $\sigma_0 = 1$, $\alpha = 10°$, $\theta_0 = 10°$, $\gamma = 0°$, and $\gamma' = 45°$ and varying t (solid curves). The dashed curves describe their no-CDW counterparts. The comparison makes it possible to isolate the CDW-related peculiarities. One sees that CDWs strengthen the differential gap features emerging at $t > 0$ for one V polarity and results in the overall CVC asymmetry.

For the configuration $N = 2$, $\sigma_0 = 1$, $\alpha = 10°$, $\theta_0 = 10°$, $\gamma = 0°$, and $\gamma' = 90°$, the distinction between the no-CDW and SCDW conductances is also substantial (see figure 14(b)). In particular, a strong complicated sub-gap structure is observed rather than the conventional logarithmic peak near $V = 0$, the outer gap edges being slightly shifted.

If the parent electron–hole pairing strength noticeably exceeds that for the Cooper pairing ($\sigma_0 = 1.3$), the resulting CVCs are similar but with the shifted singularity locations, as is shown in figure 15. In particular, the dSCDW conductances for the configuration $N = 2$, $\sigma_0 = 1.3$, $\alpha = 10°$, $\theta_0 = 10°$, $\gamma = 0°$, and $\gamma' = 90°$ has not much in common with their no-CDW counterparts. Thermally excited quasiparticles lead to huge positive and negative peaks in the sub-gap region. The observation of such features can be considered as a smoking gun of the CDW presence in cuprate electrodes.

It is of interest to illustrate the T-evolution of CVCs in the tilted configuration $\gamma = 15°$, $\gamma' = 15°$ (see figures 9 and 10). The corresponding calculations were carried out for $\sigma_0 = 1$ and 1.3 in the case of checkerboard CDWs (see figure 16). One can readily see that the peaks of the CVCs are closely located at $T = 0$, but move apart with the increase of t. A zero-bias singularity appears simultaneously. Only small remnants of the CDWs are persistent above T_c. The behavior of $G(V)$ in the cases $\sigma_0 = 1$ (panel (a)) and 1.3 (panel (b)) is analogous, except for the initial distance between two kinds of coherent peaks.

4. Conclusions

The tunnel conductances $G(V)$ were calculated for the coherent quasiparticle current flowing in the *ab*-plane of the layered partially CDW-gapped superconductors with the *d*-wave superconducting order parameter. The tunnel directionality was demonstrated to be an extremely important factor in this experimental setup. It was shown that, even in the absence of CDWs (break junctions made of pure *d*-wave BCS superconductors), the CVCs may drastically vary depending on the rotation angles γ and γ' of the crystalline electrodes. The superimposed CDW-induced features make the CVCs even more involved. Although formally the BJs are symmetric, CDWs make the CVCs highly asymmetric, which is in agreement with the experiment for cuprates. It was demonstrated that break junctions made of cuprates or related materials may be considered as a detector of CDWs. The checkerboard and unidirectional CDWs result in different forms of $G(V)$. The adopted approach was discussed here mostly as applicable to high-T_c oxides, for which plenty of data are available. However, the model is quite general and can be further modified to describe other layered CDW *d*-wave superconductors. Since layered CDW superconductors are very common [6–8, 42, 234, 235], the main task is to find proper materials, where the order parameter symmetry is truly the *d*-wave one.

Acknowledgments

The work was partially supported by the Project N 24 of the 2015–2017 Scientific Cooperation Agreement between Poland and Ukraine. T.E. also acknowledges Grant-in-Aid for Scientific Research (19540370, 245403770) from JSPS, Japan, and M.S.L. acknowledges the Narodowe Centrum Nauki in Poland (grant No 2015/19/B/ST4/02721).

ORCID iDs

A I Voitenko https://orcid.org/0000-0002-0239-7027

References

[1] Becca F, Tarquini M, Grilli M and Di Castro C 1996 *Phys. Rev.* B **54** 12443
[2] Markiewicz R S 1997 *J. Phys. Chem. Sol.* **58** 1179
[3] Dagotto E 1999 *Rep. Prog. Phys.* **62** 1525
[4] Gabovich A M and Voitenko A I 2000 *Low Temp. Phys.* **26** 305
[5] Gabovich A M, Voitenko A I, Annett J F and Ausloos M 2001 *Supercond. Sci. Technol.* **14** R1
[6] Gabovich A M, Voitenko A I and Ausloos M 2002 *Phys. Rep.* **367** 583
[7] Gabovich A M, Voitenko A I, Ekino T, Li M S, Szymczak H and Pękała M 2010 *Adv. Condens. Matter Phys.* **2010** 681070
[8] Klemm R A 2012 *Layered Superconductors* vol 1 (Oxford: Oxford University Press)
[9] Monceau P 2012 *Adv. Phys.* **61** 325
[10] Platt C, Hanke W and Thomale R 2013 *Adv. Phys.* **62** 453
[11] Gabovich A M and Voitenko A I 2013 *Fiz. Nizk. Temp.* **39** 301
[12] Spałek J 2015 *Phil. Mag.* **95** 661
[13] Fradkin E, Kivelson S A and Tranquada J M 2015 *Rev. Mod. Phys.* **87** 457
[14] Wolowiec C T, White B D and Maple M B 2015 *Physica* C **514** 113
[15] Klemm R A 2015 *Physica* C **514** 86
[16] Sebastian S E and Proust C 2015 *Annu. Rev. Condens. Matter Phys.* **6** 411
[17] Kloss T, Montiel X, de Carvalho V S, Freire H and Pépin C 2016 *Rep. Prog. Phys.* **79** 084507
[18] Hüfner S, Hossain M A, Damascelli A and Sawatzky G A 2008 *Rep. Prog. Phys.* **71** 062501
[19] Kamusella S, Doan P, Goltz T, Luetkens H, Sarkar R, Guloy A and Klauss H-H 2009 *J. Phys.: Conf. Ser.* **551** 012026
[20] Hashimoto M, Vishik I M, He R-H, Devereaux T P and Shen Z-X 2014 *Nat. Phys.* **10** 483
[21] Keimer B, Kivelson S A, Norman M R, Uchida S and Zaanen J 2015 *Nature* **518** 179
[22] Kordyuk A A 2015 *Fiz. Nizk. Temp.* **41** 417
[23] Krasnov V M 2015 *Phys. Rev.* B **91** 224508
[24] Chen C-W, Choe J and Morosan E 2016 *Rep. Prog. Phys.* **79** 084505
[25] Cea P 2016 *Eur. Phys. J.* B **89** 176
[26] Stewart G R 2011 *Rev. Mod. Phys.* **83** 1589
[27] Kordyuk A A 2012 *Fiz. Nizk. Temp.* **38** 1119
[28] Fernandes R M, Chubukov A V and Schmalian J 2014 *Nat. Phys.* **10** 97
[29] Chubukov A and Hirschfeld P J 2015 *Phys. Today* **68** 46
[30] Sugimoto A, Sakai Y, Nagasaka K and Ekino T 2015 *Physica* C **518** 23
[31] Martinelli A, Bernardini F and Massidda S 2016 *C. R. Phys.* **17** 5
[32] Inosov D S 2016 *C. R. Phys.* **17** 60
[33] Fernandes R M and Chubukov A V 2017 *Rep. Prog. Phys.* **80** 014503
[34] Wilson J A, Di Salvo F J and Mahajan S 1975 *Adv. Phys.* **24** 117
[35] Friend R H and Yoffe A D 1987 *Adv. Phys.* **36** 1
[36] Borisenko S V *et al* 2009 *Phys. Rev. Lett.* **102** 166402
[37] Weber F, Rosenkranz S, Heid R and Said A H 2016 *Phys. Rev.* B **94** 140504
[38] Liu Y *et al* 2016 *Phys. Rev.* B **94** 045131
[39] Maschek M *et al* 2016 *Phys. Rev.* B **94** 214507
[40] Novello A M, Spera M, Scarfato A, Ubaldini A, Giannini E, Bowler D R and Renner C 2017 *Phys. Rev. Lett.* **118** 017002
[41] Kogar A *et al* 2017 *Phys. Rev. Lett.* **118** 027002
[42] Wang B, Liu Y, Ishigaki K, Matsubayashi K, Cheng J, Lu W, Sun Y and Uwatoko Y 2017 *Phys. Rev.* B **95** 220501
[43] Friend R H and Jérome D 1979 *J. Phys. C: Solid State Phys.* **12** 1441
[44] Littlewood P B and Heine V 1981 *J. Phys. C: Solid State Phys.* **14** 2943
[45] Roth S and Carroll D 2004 *One-Dimensional Metals* (Weinheim: Wiley)
[46] van Wezel J, Nahai-Williamson P and Saxena S S 2010 *Europhys. Lett.* **89** 47004
[47] Cho D, Cho Y-H, Cheong S-W, Kim K-S and Yeom H W 2015 *Phys. Rev.* B **92** 085132
[48] Maschek M, Rosenkranz S, Heid R, Said A H, Giraldo-Gallo P, Fisher I R and Weber F 2015 *Phys. Rev.* B **91** 235146
[49] Thampy V *et al* 2017 *Phys. Rev.* B **95** 241111
[50] Chang J *et al* 2012 *Nat. Phys.* **8** 751
[51] LeBoeuf D, Krämer S, Hardy W N, Liang R, Bonn D A and Proust C 2013 *Nat. Phys.* **9** 79
[52] Tabis W *et al* 2014 *Nat. Commun.* **5** 5875
[53] Doiron-Leyraud N 2015 *Nat. Commun.* **6** 6034
[54] Comin R, Sutarto R, da Silva Neto E H, Chauviere L, Liang R, Hardy W N, Bonn D A, He F, Sawatzky G A and Damascelli A 2015 *Science* **347** 1335
[55] Wu T, Mayaffre H, Krämer S, Horvatić M, Berthier C, Hardy W N, Liang R, Bonn D A and Julien M-H 2015 *Nat. Commun.* **6** 6438
[56] Comin R *et al* 2015 *Nat. Mater.* **14** 796
[57] Forgan E M *et al* 2015 *Nat. Commun.* **5** 10064
[58] Cyr-Choinière O, Grissonnanche G, Badoux S, Day J, Bonn D A, Hardy W N, Liang R, Doiron-Leyraud N and Taillefer L 2015 *Phys. Rev.* B **92** 224502
[59] Gerber S *et al* 2015 *Science* **350** 949
[60] Kharkov Y A and Sushkov O P 2016 *Sci. Rep.* **6** 34551
[61] Peng Y Y 2016 *Phys. Rev.* B **94** 184511
[62] Zheng Y, Fei Y, Bu K, Zhang W, Ding Y, Zhou X, Hoffman J E and Yin Y 2017 *Sci. Rep.* **7** 8059
[63] Hoffman J E, Hudson E W, Lang K M, Madhavan V, Eisaki H, Uchida S and Davis J C 2002 *Science* **295** 466
[64] Kurosawa T *et al* 2015 *Int. J. Mod. Phys.* B **29** 1542009
[65] Mesaros A, Fujita K, Edkins S D, Hamidian M H, Eisaki H, Uchida S-I, Davis J C S, Lawler M J and Kim E-A 2016 *Proc. Natl Acad. Sci. USA* **113** 12661
[66] Chaix L *et al* 2017 *Nat. Phys.* **13** 952
[67] da Silva Neto E H, Comin R, He F, Sutarto R, Jiang Y, Greene R L, Sawatzky G A and Damascelli A 2015 *Science* **347** 282
[68] Phillips J C, Saxena A and Bishop A R 2003 *Rep. Prog. Phys.* **66** 2111
[69] Mostovoy M V, Marchetti F M, Simons B D and Littlewood P B 2005 *Phys. Rev.* B **71** 224502
[70] Pasupathy A N, Pushp A, Gomes K K, Parker C V, Wen J, Xu Z, Gu G, Ono S, Ando Y and Yazdani A 2008 *Science* **320** 196
[71] Poccia N, Lankhorst M and Golubov A A 2014 *Physica* C **503** 82
[72] Achkar A J, Mao X, McMahon C, Sutarto R, He F, Liang R, Bonn D A, Hardy W N and Hawthorn D G 2014 *Phys. Rev. Lett.* **113** 107002
[73] Carlson E W, Liu S, Phillabaum B and Dahmen K A 2015 *J. Supercond.* **28** 1237
[74] Honma T and Hor P H 2015 *Physica* C **509** 11
[75] Shengelaya A and Müller K A 2015 *Europhys. Lett.* **109** 27001
[76] Campi G *et al* 2015 *Nature* **525** 359
[77] Campi G and Bianconi A 2016 *J. Supercond.* **29** 627
[78] Vojta M 2009 *Adv. Phys.* **58** 699
[79] Giannetti C, Capone M, Fausti D, Fabrizio M, Parmigiani F and Mihailovic D 1991 *Adv. Phys.* **65** 58
[80] Caprara S, Di Castro C, Seibold G and Grilli M 2017 *Phys. Rev.* B **95** 224511

[81] Rice T M 2017 *Phil. Mag.* **97** 360
[82] Gabovich A M and Voitenko A I 2007 *Phys. Rev.* B **75** 064516
[83] Gabovich A M and Voitenko A I 2014 *Physica* C **503** 7
[84] Gabovich A M and Voitenko A I 2016 *Fiz. Nizk. Temp.* **42** 1103
[85] Ekino T, Gabovich A M, Li M S, Szymczak H and Voitenko A I 2016 *J. Phys.: Condens. Matter* **28** 445701
[86] Kirtley J R 1990 *Int. J. Mod. Phys.* B **4** 201
[87] Fang A, Howald C, Kaneko N, Greven M and Kapitulnik A 2004 *Phys. Rev.* B **70** 214514
[88] Boyer M C, Wise W D, Chatterjee K, Yi M, Kondo T, Takeuchi T, Ikuta H and Hudson E W 2007 *Nat. Phys.* **3** 802
[89] Gomes K K, Pasupathy A N, Pushp A, Ono S, Ando Y and Yazdani A 2007 *Physica C* **460–2** 212
[90] Gomes K K, Pasupathy A N, Pushp A, Ono S, Ando Y and Yazdani A 2007 *Nature* **447** 569
[91] Yazdani A 2009 *J. Phys.: Condens. Matter* **21** 164214
[92] Kato T, Funahashi H, Nakamura H, Fujimoto M, Machida T, Sakata H, Nakao S and Hasegawa T 2010 *J. Supercond.* **23** 771
[93] Alldredge J W, Fujita K, Eisaki H, Uchida S and McElroy K 2013 *Phys. Rev.* B **87** 104520
[94] Sugimoto A, Ekino T, Tanaka K, Mineta K, Tanabe K and Tokiwa K 2014 *Phys. Proced.* **58** 78
[95] Fischer Ø, Kugler M, Maggio-Aprile I and Berthod C 2007 *Rev. Mod. Phys.* **79** 353
[96] Kordyuk A A *et al* 2009 *Phys. Rev.* B **79** 020504
[97] Tajima S 2016 *Rep. Prog. Phys.* **79** 094001
[98] Stewart G R 2017 *Adv. Phys.* **66** 75
[99] Kabanov V V, Demsar J and Mihailovic D 2000 *Phys. Rev.* B **61** 1477
[100] Demsar J, Forró L, Berger H and Mihailovic D 2002 *Phys. Rev.* B **66** 041101
[101] Mihailovic D 2005 *Phys. Rev. Lett.* **94** 207001
[102] Muller K A and Bussmann-Holder A (ed) 2005 *Superconductivity in Complex Systems* (*Structure and Bonding* vol 114) (Berlin: Springer)
[103] Stojchevska L, Vaskivskyi I, Mertelj T, Kusar P, Svetin D, Brazovskii S and Mihailovic D 2014 *Science* **344** 177
[104] Vaskivskyi I, Mihailovic I A, Brazovskii S, Gospodaric J, Mertelj T, Svetin D, Sutar P and Mihailovic D 2016 *Nat. Commun.* **7** 11442
[105] Moreland J and Ekin J W 1985 *J. Appl. Phys.* **58** 5888
[106] Ekino T, Takabatake T, Tanaka H and Fujii H 1995 *Phys. Rev. Lett.* **75** 4262
[107] Ekino T, Doukan T and Fujii H 1996 *J. Low Temp. Phys.* **105** 563
[108] Keijsers R J P, Shklyarevskii O I, Hermsen J G H and van Kempen H 1996 *Rev. Sci. Instrum.* **67** 2863
[109] Cucolo A M, Bobba F and Akimenko A I 2000 *Phys. Rev.* B **61** 694
[110] Mourachkine A 2000 *J. Supercond.* **13** 101
[111] Ekino T, Takasaki T, Muranaka T, Akimitsu J and Fujii H 2003 *Phys. Rev.* B **67** 094504
[112] Shanygina T E *et al* 2011 *Pis'ma Zh. Éksp. Teor. Fiz.* **93** 95
[113] Ekino T, Sugimoto A, Sakai Y, Gabovich A M and Akimitsu J 2014 *Fiz. Nizk. Temp.* **40** 1182
[114] Kuzmichev S A and Kuzmicheva T E 2016 *Fiz. Nizk. Temp.* **42** 1284
[115] Tsuei C C and Kirtley J R 2000 *Rev. Mod. Phys.* **72** 969
[116] Hilgenkamp H and Mannhart J 2002 *Rev. Mod. Phys.* **74** 485
[117] Kirtley J R, Tsuei C C, Ariando A, Verwijs C J M, Harkema S and Hilgenkamp H 2006 *Nat. Phys.* **2** 190
[118] Kirtley J R 2011 *C. R. Phys.* **12** 436
[119] Sun A G, Gajewski D A, Maple M B and Dynes R C 1994 *Phys. Rev. Lett.* **72** 2267
[120] Klemm R A 2005 *Phil. Mag.* **85** 801
[121] Kimura H, Barber R P Jr, Ono S, Ando Y and Dynes R C 2009 *Phys. Rev.* B **80** 144506
[122] Kashiwagi T 2015 *Appl. Phys. Lett.* **107** 082601
[123] Ponomarev Y G, Van H H, Kuzmichev S A, Kulbachinskii S V, Mikheev M G, Sudakova M V and Tchesnokov S N 2012 *Pis'ma Zh. Éksp. Teor. Fiz.* **96** 830
[124] Zhong Y *et al* 2016 *Sci. Bull.* **61** 1239
[125] Lee W S, Vishik I M, Tanaka K, Lu D H, Sasagawa T, Nagaosa N, Devereaux T P, Hussain Z and Shen Z-X 2007 *Nature* **450** 81
[126] Hüfner S and Müller F 2008 *Phys. Rev.* B **78** 014521
[127] Kondo T, Khasanov R, Takeuchi T, Schmalian J and Kaminski A 2009 *Nature* **457** 296
[128] Kurosawa T *et al* 2010 *Phys. Rev.* B **81** 094519
[129] Vishik I M, Lee W S, He R-H, Hashimoto M, Hussain Z, Devereaux T P and Shen Z-X 2010 *New J. Phys.* **12** 105008
[130] Vishik I M *et al* 2012 *Proc. Natl Acad. Sci. USA* **109** 18332
[131] Hüfner S and Müller F 2012 *Physica* C **483** 165
[132] Kondo T, Palczewski A D, Hamaya Y, Takeuchi T, Wen J S, Xu Z J, Gu G and Kaminski A 2013 *Phys. Rev. Lett.* **111** 157003
[133] Kondo T, Malaeb W, Ishida Y, Sasagawa T, Sakamoto H, Takeuchi T, Tohyama T and Shin S 2015 *Nat. Commun.* **6** 7699
[134] Kaminski A, Kondo T, Takeuchi T and Gu G 2015 *Phil. Mag.* **95** 453
[135] Yazdani A, da Silva Neto E H and Aynajian P 2016 *Annu. Rev. Condens. Matter Phys.* **7** 11
[136] Mandrus D, Forro L, Koller D and Mihaly L 1991 *Nature* **351** 460
[137] Ekino T, Sezaki Y and Fujii H 1999 *Phys. Rev.* B **60** 6916
[138] Ekino T, Hashimoto S, Takasaki T and Fujii H 2001 *Phys. Rev.* B **64** 092510
[139] Vedeneev S I and Maude D K 2005 *Phys. Rev.* B **72** 144519
[140] Tafuri F and Kirtley J R 2005 *Rep. Prog. Phys.* **68** 2573
[141] Kirtley J R and Tafuri F 2007 *Handbook of High-Temperature Superconductivity. Theory and Experiment* ed J R Schrieffer and J S Brooks (New York: Springer) p 19
[142] Tafuri F *et al* 2013 *J. Supercond.* **26** 21
[143] Kulik I O and Yanson I K 1971 *Josephson Effect in Superconducting Tunneling Structures* (New York: Coronet)
[144] Wolf E L 1985 *Principles of Electron Tunneling Spectroscopy* (New York: Oxford University Press)
[145] Ledvij M and Klemm R A 1995 *Phys. Rev.* B **51** 3269
[146] Daghero D, Tortello M, Pecchio P, Stepanov V A and Gonnelli R S 2013 *Fiz. Nizk. Temp.* **39** 261
[147] Gabovich A M, Li M S, Szymczak H and Voitenko A I 2013 *Phys. Rev.* B **87** 104503
[148] Ekino T, Gabovich A M, Li M S, Pękała M, Szymczak H and Voitenko A I 2011 *J. Phys.: Condens. Matter* **23** 385701
[149] Giaever I 1974 *Rev. Mod. Phys.* **46** 245
[150] Won H and Maki K 1994 *Phys. Rev.* B **49** 1397
[151] Wu J, Bollinger A T, He X and Božović I 2017 *Nature* **547** 432
[152] Bilbro G and McMillan W L 1976 *Phys. Rev.* B **14** 1887
[153] Gabovich A M, Li M S, Szymczak H and Voitenko A I 2003 *J. Phys.: Condens. Matter* **15** 2745
[154] Ekino T, Gabovich A M, Li M S, Pękała M, Szymczak H and Voitenko A I 2011 *Symmetry* **3** 699
[155] Gabovich A M, Li M S, Szymczak H and Voitenko A I 2015 *Phys. Rev.* B **92** 054512
[156] Ye G Z *et al* 2016 *Phys. Rev.* B **94** 224508
[157] Helm T *et al* 2017 *Phys. Rev.* B **95** 075121
[158] Denholme S J, Yukawa A, Tsumura K, Nagao M, Tamura R, Watauchi S, Tanaka I, Takayanagi H and Miyakawa N 2017 *Sci. Rep.* **7** 45217

[159] Ren M Q *et al* 2017 *Phil. Mag.* **97** 527
[160] Peierls R E 1955 *Quantum Theory of Solids* (Oxford: Clarendon)
[161] Rossnagel K 2011 *J. Phys.: Condens. Matter* **23** 213001
[162] Hellmann S 2012 *Nat. Commun.* **3** 1069
[163] Zhu X, Guo J, Zhang J and Plummer E W 2017 *Adv. Phys.* X **2** 622
[164] Halperin B I and Rice T M 1968 *Solid State Phys.* **21** 115
[165] Kopaev Y V 1975 *Tr. Fiz. Inst. Akad. Nauk SSSR* **86** 3
[166] Ginzburg V L (ed) 1987 *Superconductivity, Superdiamagnetism, Superfluidity* (Moscow: Mir)
[167] Keimer B 2013 *Emergent Phenomena in Correlated Matter Modeling and Simulation* vol 3, ed E Pavarini *et al* (Jülich: Forschungszentrum Jülich) p 9.1
[168] Le Tacon M, Bosak A, Souliou S M, Dellea G, Loew T, Heid R, Bohnen K-P, Ghiringhelli G, Krisch M and Keimer B 2014 *Nat. Phys.* **10** 52
[169] Först M *et al* 2014 *Phys. Rev.* B **90** 184514
[170] Coleman R V, Giambattista B, Hansma P K, Johnson A, Mcnairy W W and Slough C G 1988 *Adv. Phys.* **37** 559
[171] Whangbo M-H, Canadell E, Foury P and Pouget J-P 1991 *Science* **252** 96
[172] Gweon G-H, Allen J W, Clack J A, Zhang Y X, Poirier D M, Benning P J, Olson C G, Marcus J and Schlenker C 1997 *Phys. Rev.* B **55** 13353
[173] Kolincio K K, Pérez O, Hébert S, Fertey P and Pautrat A 2016 *Phys. Rev.* B **93** 235126
[174] Afanas'ev A M and Kagan Y 1962 *Zh. É ksp. Teor. Fiz.* **43** 1456
[175] Chan S-K and Heine V 1973 *J. Phys. F: Met. Phys.* **3** 795
[176] Johannes M D, Mazin I I and Howells C A 2006 *Phys. Rev.* B **73** 205102
[177] Johannes M D and Mazin I I 2008 *Phys. Rev.* B **77** 165135
[178] White R M 2007 *Quantum Theory of Magnetism* (Berlin: Springer)
[179] Kohn W 1959 *Phys. Rev. Lett.* **2** 393
[180] Klemm R A 2000 *Physica* C **341–8** 839
[181] Borisenko S V *et al* 2008 *Phys. Rev. Lett.* **100** 196402
[182] Kordyuk A A, Zabolotnyy V B, Evtushinsky D V, Bü chner B and Borisenko S V 2010 *J. Electron Spectrosc. Relat. Phenom.* **181** 44
[183] Tinkham M 2004 *Introduction to Superconductivity* (Mineola, NY: Dover)
[184] Damascelli A, Hussain Z and Shen Z-X 2003 *Rev. Mod. Phys.* **75** 473
[185] Tabis W *et al* 2017 *Phys. Rev.* B **96** 134510
[186] Mandrus D, Hartge J, Kendziora C, Mihaly L and Forro L 1993 *Europhys. Lett.* **22** 199
[187] Ponomarev Y G *et al* 1995 *Physica* C **243** 167
[188] Hartge J, Forr L, Mandrus D, Martin M C, Kendziora C and Mihaly L 1993 *J. Phys. Chem. Sol.* **54** 1359
[189] Larkin A I and Ovchinnikov Y N 1966 *Sov. Phys.—JETP* **24** 1035
[190] Gabovich A M, Pashitskii E A and Shpigel A S 1976 *Sov. Phys. Solid State* **18** 1911
[191] Barone A and Paterno G 1982 *The Physics and Applications of the Josephson Effect* (New York: Wiley)
[192] Gabovich A M 1992 *Sov. J. Low Temp. Phys.* **18** 490
[193] Gabovich A M and Voitenko A I 1995 *Phys. Rev.* B **52** 7437
[194] Gabovich A M and Voitenko A I 1997 *Phys. Rev.* B **55** 1081
[195] Gabovich A M and Voitenko A I 1997 *J. Phys.: Condens. Matter* **9** 3901
[196] Voitenko A I and Gabovich A M 2007 *Fiz. Tverd. Tela* **49** 1356
[197] Ekino T, Gabovich A M, Li M S, Pękała M, Szymczak H and Voitenko A I 2008 *J. Phys.: Condens. Matter* **20** 425218
[198] Cohen M H, Falicov L M and Phillips J C 1962 *Phys. Rev. Lett.* **8** 316
[199] Artemenko S N and Volkov A F 1984 *Sov. Phys.—JETP* **60** 395
[200] Bruder C, van Otterlo A and Zimanyi G T 1995 *Phys. Rev.* B **51** 12904
[201] Barash Y S, Galaktionov A V and Zaikin A D 1995 *Phys. Rev.* B **52** 665
[202] Barash Y S, Burkhardt H and Rainer D 1996 *Phys. Rev. Lett.* **77** 4070
[203] Nie Y-M and Coffey L 1998 *Phys. Rev.* B **57** 3116
[204] Nie Y-M and Coffey L 1999 *Phys. Rev.* B **59** 11982
[205] Gabovich A M and Voitenko A I 2012 *Fiz. Nizk. Temp.* **38** 414
[206] Gabovich A M, Li M S, Szymczak H and Voitenko A I 2014 *Eur. Phys. J.* B **87** 115
[207] Gabovich A M, Voitenko A I, Li M S and Szymczak H 2015 *Physica* C **516** 62
[208] Barash Y S, Galaktionov A V and Zaikin A D 1995 *Phys. Rev. Lett.* **75** 1676
[209] Sommerfeld A and Bethe H 1933 *Elektronentheorie der Metalle* (Berlin: Springer)
[210] Frenkel J 1930 *Phys. Rev.* **36** 1604
[211] Ekino T, Fujii H, Kosugi M, Zenitani Y and Akimitsu J 1996 *Phys. Rev.* B **53** 5640
[212] D'yachenko A I, Tarenkov V Y, Szymczak R, Szymczak H, Abal'oshev A V, Lewandowski S J and Leonyuk L 2003 *Fiz. Nizk. Temp.* **29** 149
[213] Takasaki T, Ekino T, Sugimoto A, Shohara K, Yamanaka S and Gabovich A M 2010 *Eur. Phys. J.* B **73** 471
[214] Renner C and Fischer Ø 1995 *Phys. Rev.* B **51** 9208
[215] DeWilde Y *et al* 1998 *Phys. Rev. Lett.* **80** 153
[216] Cren T, Roditchev D, Sacks W, Klein J, Moussy J-B, Deville-Cavellin C and Laguës M 2000 *Phys. Rev. Lett.* **84** 147
[217] Ozyuzer L, Zasadzinski J F, Gray K E, Hinks D G and Miyakawa N 2003 *IEEE Trans. Appl. Supercond.* **13** 893
[218] Sugimoto A, Shohara K, Ekino T, Watanabe Y, Harada Y, Mikusu S, Tokiwa K and Watanabe T 2009 *Physica* C **469** 1020
[219] Sugimoto A, Ekino T, Gabovich A M, Sekine R, Tanabe K and Tokiwa K 2017 *Phys. Rev.* B **95** 174508
[220] Ekino T, Doukan T, Fujii H, Nakamura F, Sakita S, Kodama M and Fujita T 1996 *Physica* C **263** 249
[221] Ekino T, Sezaki Y, Hashimoto S and Fujii H 1999 *J. Low Temp. Phys.* **117** 359
[222] Mourachkine A 2000 *Europhys. Lett.* **49** 86
[223] Giubileo F, Jossa A, Bobba F, Akimenko A I and Cucolo A M 2001 *Eur. Phys. J.* B **24** 305
[224] Mourachkine A 2005 *Mod. Phys. Lett.* **19** 743
[225] Akimenko A I, Bobba F, Giubileo F, Gudimenko V A, Piano S and Cucolo A M 2010 *Fiz. Nizk. Temp.* **36** 212
[226] Gabovich A M and Voitenko A I 1997 *Phys. Rev.* B **56** 7785
[227] Kivelson S A, Bindloss I P, Fradkin E, Oganesyan V, Tranquada J M, Kapitulnik A and Howald C 2003 *Rev. Mod. Phys.* **75** 1201
[228] Krasnov V M, Yurgens A, Winkler D, Delsing P and Claeson T 2000 *Phys. Rev. Lett.* **84** 5860
[229] Katterwe S O, Rydh A and Krasnov V M 2008 *Phys. Rev. Lett.* **101** 087003
[230] Krasnov V M 2009 *Phys. Rev.* B **79** 214510
[231] Ozyuzer L, Zasadzinski J F and Miyakawa N 1999 *Int. J. Mod. Phys.* B **13** 3721
[232] Zasadzinski J F, Ozyuzer L, Miyakawa N, Gray K E, Hinks D G and Kendziora C 2001 *Phys. Rev. Lett.* **87** 067005
[233] Tonouchi D, Matsushita M M and Awaga K 2017 *Phys. Rev.* B **96** 045116
[234] Pribulová Z *et al* 2017 *Phys. Rev.* B **95** 174512
[235] Cao G, Xie W, Phelan W A, DiTusa J F and Jin R 2017 *Phys. Rev.* B **95** 035148